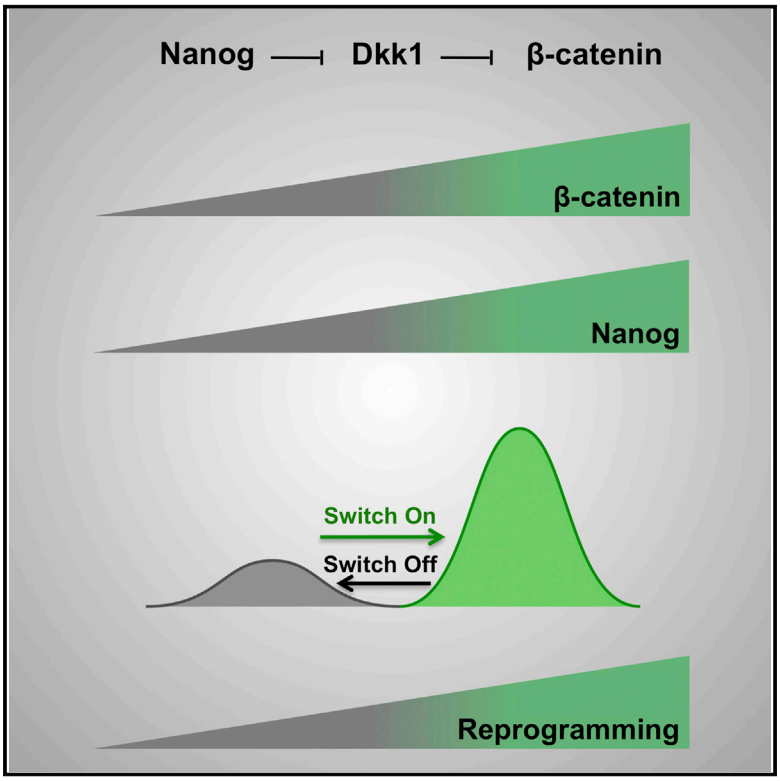
Report

Cell Reports

β-Catenin Fluctuates in Mouse ESCs and Is Essential for Nanog-Mediated Reprogramming of Somatic Cells to Pluripotency

Graphical Abstract



Highlights

Nanog activates the Wnt pathway by repressing Dkk1

Nanog enhances reprogramming by activating the Wnt pathway

β-Catenin fluctuates in ESCs following Nanog dynamics in serum+LIF medium

β-Catenin is metastable in ESCs cultured in serum+LIF and in 2i+LIF media

Authors

Lucia Marucci, Elisa Pedone, ..., Mark Isalan, Maria Pia Cosma

Correspondence

pia.cosma@crg.es

In Brief

Embryonic stem cell (ESC) pluripotency is controlled by a network of transcription factors, which includes Nanog, and by the Wnt /β-catenin pathway. In this study, Marucci et al. show that repression of Dkk1 by Nanog is essential for Nanog-mediated reprogramming of somatic cells. β-Catenin and Nanog exhibit correlated heterogeneity, fluctuating synchronously in ESCs cultured in serum plus leukemia inhibitory factor (LIF). Instead, β-catenin fluctuations are independent of Nanog in 2i+LIF, a medium that favors pluripotency and loss of mosaic expression of stem genes.

Marucci et al., 2014, Cell Reports 8, 1–11
September 25, 2014 ©2014 The Authors
http://dx.doi.org/10.1016/j.celrep.2014.08.011

CellPress

Please cite this article in press as: Marucci et al., β-Catenin Fluctuates in Mouse ESCs and Is Essential for Nanog-Mediated Reprogramming of Somatic Cells to Pluripotency, Cell Reports (2014), http://dx.doi.org/10.1016/j.celrep.2014.08.011

Cell Reports
Report

OPEN ACCESS
CellPress

β-Catenin Fluctuates in Mouse ESCs and Is Essential for Nanog-Mediated Reprogramming of Somatic Cells to Pluripotency

Lucia Marucci,[1,2,4] Elisa Pedone,[1,4] Umberto Di Vicino,[1] Blanca Sanuy-Escribano,[1] Mark Isalan,[1,5] and Maria Pia Cosma[1,3,*]
[1]Centre for Genomic Regulation (CRG), 08003 Barcelona, Spain
[2]Department of Engineering Mathematics, University of Bristol, Bristol BS8 1UB, UK
[3]Institució Catalana de Recerca i Estudis Avançats (ICREA), 08010 Barcelona, Spain
[4]Co-first author
[5]Present address: Department of Life Sciences, Imperial College London, London SW7 2AZ, UK
*Correspondence: pia.cosma@crg.es
http://dx.doi.org/10.1016/j.celrep.2014.08.011
This is an open access article under the CC BY-NC-ND license (http://creativecommons.org/licenses/by-nc-nd/3.0/).

SUMMARY

The Wnt/β-catenin pathway and Nanog are key regulators of embryonic stem cell (ESC) pluripotency and the reprogramming of somatic cells. Here, we demonstrate that the repression of Dkk1 by Nanog, which leads indirectly to β-catenin activation, is essential for reprogramming after fusion of ESCs overexpressing Nanog. In addition, β-catenin is necessary in Nanog-dependent conversion of preinduced pluripotent stem cells (pre-iPSCs) into iPSCs. The activation of β-catenin by Nanog causes fluctuations of β-catenin in ESCs cultured in serum plus leukemia inhibitory factor (serum+LIF) medium, in which protein levels of key pluripotency factors are heterogeneous. In 2i+LIF medium, which favors propagation of ESCs in a ground state of pluripotency with many pluripotency genes losing mosaic expression, we show Nanog-independent β-catenin fluctuations. Overall, we demonstrate Nanog and β-catenin cooperation in establishing naive pluripotency during the reprogramming process and their correlated heterogeneity in ESCs primed toward differentiation.

INTRODUCTION

The activation of the Wnt signaling pathway enhances embryonic stem cell (ESC) self-renewal and reprogramming of somatic cells to pluripotency (Kühl and Kühl, 2013; Lluis et al., 2008; Marson et al., 2008; Sato et al., 2004; Sokol, 2011). β-Catenin is the key effector of this pathway, and its stability is modulated by the destruction complex, which is formed by Gsk3, Axin, APC, and CK1 (Stamos and Weis, 2013). Dickkopf-related protein 1 (Dkk1) is one of the β-catenin targets, and it binds the LRP-5/6 Wnt coreceptor to prevent the binding of its ligand (Kawano and Kypta, 2003).

Mouse ESCs are transcriptionally heterogeneous. In serum plus leukemia inhibitory factor (serum+LIF) medium, Esrrb (van den Berg et al., 2008), Stella (Hayashi et al., 2008), Nanog, zinc-finger protein 42, T box 3, and Klf4 show metastable protein expression levels (Cahan and Daley, 2013). In contrast, in ESCs cultured in 2i+LIF medium, which include Mek and GSK3 inhibitors (Ying et al., 2008), the expression profile is homogeneous (Marks et al., 2012; Wray et al., 2010).

Nanog is a key factor in the ESC core pluripotency network and is necessary for maintenance of the naive pluripotent state of ESCs (Chambers et al., 2003; Loh et al., 2006; Mitsui et al., 2003). Overexpression of Nanog enhances cell-fusion-mediated reprogramming (Silva et al., 2006) and is essential for conversion of preinduced pluripotent stem cells (pre-iPSCs) to fully reprogrammed iPSCs (Silva et al., 2009).

Here, we demonstrate that Nanog controls β-catenin through direct inhibition of Dkk1, which results in β-catenin accumulation in ESCs overexpressing Nanog. β-Catenin is essential for reprogramming of somatic cells after their fusion with Nanog-overexpressing ESCs and for the conversion of pre-iPSCs into iPSCs, when Nanog establishes naive pluripotency during the reprogramming process.

Furthermore, we show that β-catenin fluctuates synchronously with Nanog in mouse ESCs cultured in serum+LIF, while its fluctuations in 2i+LIF are independent of Nanog. We derived a differential equation-based model that captures Nanog and β-catenin fluctuations with bistable dynamics.

RESULTS

Nanog Regulates the Wnt/β-Catenin Pathway by Repressing Dkk1

ESC pluripotency is regulated by a network of signaling pathways and transcription factors. We examined the functional correlation between Nanog and β-catenin activities in ESCs.

First, we investigated Wnt pathway activity in ESCs that overexpress Nanog (EF4 cells) (Silva et al., 2006) and in ESC mutants lacking one Nanog allele (Nanog βgeo/+ cells) (Mitsui et al., 2003). EF4 cells accumulated high levels of β-catenin,

Please cite this article in press as: Marucci et al., β-Catenin Fluctuates in Mouse ESCs and Is Essential for Nanog-Mediated Reprogramming of Somatic Cells to Pluripotency, Cell Reports (2014), http://dx.doi.org/10.1016/j.celrep.2014.08.011

OPEN ACCESS
CellPress

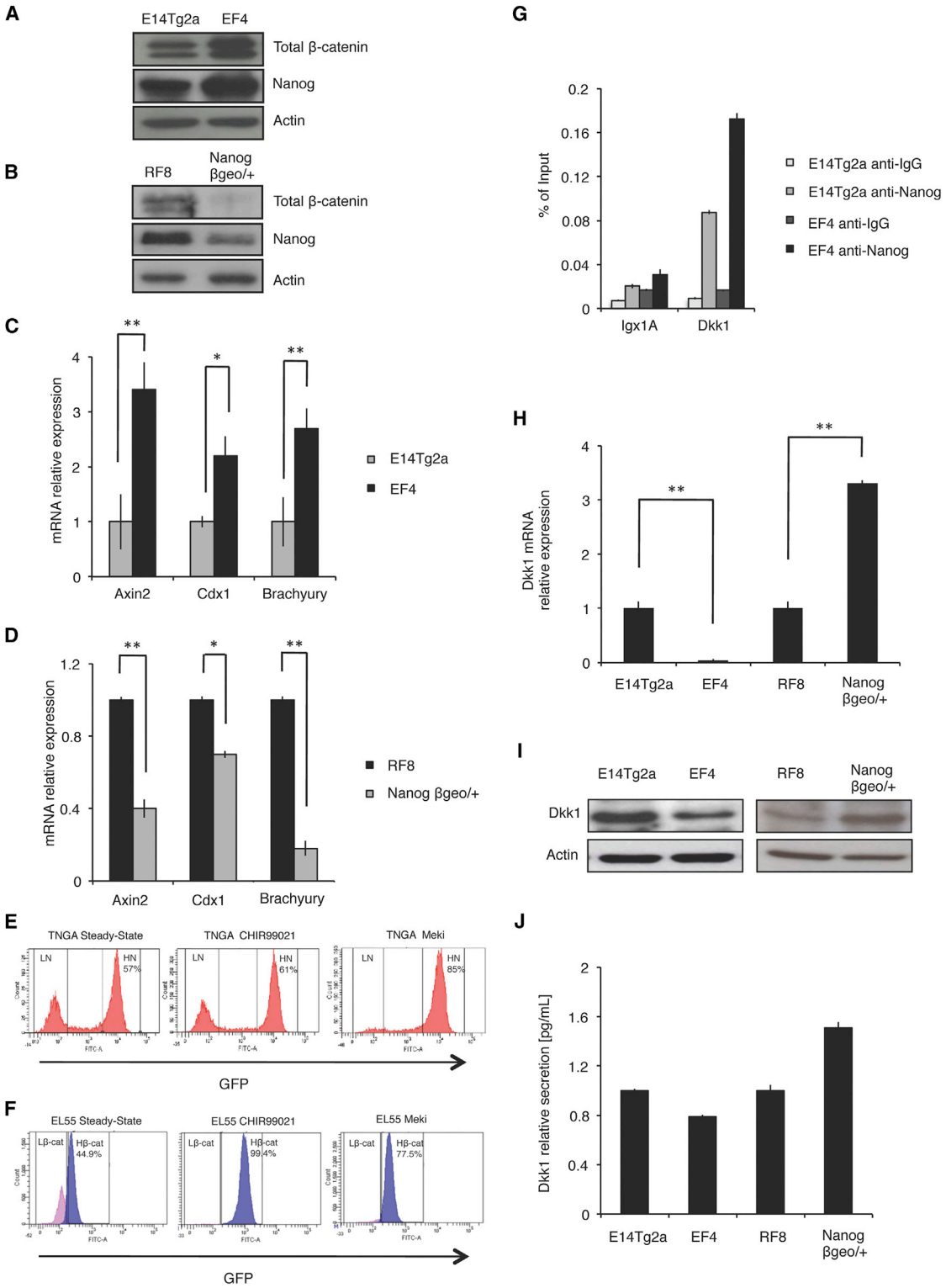


Figure 1. Nanog Stabilizes β-Catenin Levels by Inhibiting Dkk1

(A and B) Western blot of total β-catenin and Nanog in E14Tg2a, EF4 (A), RF8, and Nanog βgeo/+ cells (B).

(C and D) Quantitative PCR (qPCR) of Wnt pathway targets in E14Tg2a, EF4 (C), RF8, and Nanog βgeo/+ cells (D).

(E and F) FACS analysis of GFP distribution of TNGA and EL55 cells treated with Chiron (3 μM) for 1 day and the Mek inhibitor PD184352 (3 μM) for 7 days.

(G) Chromatin immunoprecipitation (ChIP) of Nanog on Dkk1 and Igx1A promoters in E14Tg2a and EF4 cells.

(legend continued on next page)

while Nanog βgeo/+ cells showed reduced levels, as compared to controls (E14Tg2a and RF8 cells, respectively) (Figures 1A, 1B, and S1A). The Wnt/β-catenin target genes Axin2, Cdx1, and Brachyury were expressed at higher levels in EF4 cells (Figure 1C), and at lower levels in Nanog βgeo/+ cells (Figure 1D), compared to controls. These data suggest that Nanog promotes β-catenin accumulation in ESCs. Of note, levels of Nanog were not altered in EF4 cells treated with the Wnt pathway inhibitors Dkk1 or IWP2, while β-catenin levels and activity were reduced (Figures S1B–S1D).

We next asked whether β-catenin is Nanog dependent in TNGA cells, an ESC line expressing GFP from Nanog allele (Chambers et al., 2007), and in EL55 cells, an ESC line expressing endogenous β-catenin fused with GFP (Figures S1E–S1I). GFP-tagged β-catenin colocalized and had correlated expression levels with endogenous β-catenin and did not show abnormal endosomal accumulation (Figures S1J and S1K; $r = 0.98$). Untagged and GFP-tagged forms of β-catenin in EL55 cells were increased upon activation of the Wnt pathway using the GSK3 inhibitor Chiron (CHIR99021) (Figure S1L), and β-catenin target genes were turned on by Chiron treatment (Figure S1M).

To investigate whether β-catenin is Nanog dependent, we used a Mek inhibitor (Meki) (Ying et al., 2008), which upregulates Nanog (Silva et al., 2009), and Chiron. Upon Chiron treatment, the GFP distribution in TNGA cells was unaltered, while EL55 cells became almost all GFP+ (Figures 1E and 1F, Hβ-cat). In contrast, upon Nanog induction using the Meki, both TNGA and EL55 cells became GFP+ (Figures 1E and 1F, Hβ-cat, HN), which suggested that Nanog controls β-catenin stabilization. Moreover there was no β-catenin accumulation in Nanog null cells (Nanog βgeo/Hygro) (Mitsui et al., 2003) upon Meki treatment (Figure S1N).

Dkk1 is a secreted factor (Niehrs, 2006) expressed by ESCs (Kotini et al., 2011) that prevents binding of the Wnts (Kawano and Kypta, 2003). Having observed activation of Wnt targets in EF4 cells and induction of β-catenin accumulation by Nanog, we investigated whether Nanog is a repressor of Dkk1. We show Nanog binding to the Dkk1 promoter in ESCs and increased binding in EF4 cells (Figure 1G), which suggests direct regulation of Dkk1 transcription by Nanog. Accordingly, Dkk1 mRNA and protein levels were lower in EF4 cells and higher in Nanog βgeo/+ cells compared to controls (Figures 1H and 1I). Dkk1 levels were comparable in the different cell media (Figure 1J), indicating the prevalence of its autocrine regulation of the Wnt pathway.

Overall, these data show that Nanog represses Dkk1 transcription and thereby induces indirect activation of the Wnt/β-catenin pathway by promoting β-catenin accumulation.

Nanog Enhances Cell-Fusion-Mediated Reprogramming by Increasing β-Catenin Accumulation upon Dkk1 Repression

β-Catenin accumulation and Nanog overexpression in ESCs enhance reprogramming after fusion (Lluis and Cosma, 2009; Lluis et al., 2008, 2010; Silva et al., 2006). As Nanog overexpression stabilizes β-catenin in EF4 cells through Dkk1 repression, we investigated whether reprogramming of somatic cells after EF4-cell fusion was due to Nanog in cooperation with the Wnt/β-catenin pathway. Thus, we fused NPCs-Oct4-Puro-GFP (neural precursor cells carrying the Oct4-Puro-GFP transgene) with wild-type ESCs, with EF4, and with Dkk1-treated EF4 cells (Figures 2A and S1C). GFP-positive reprogrammed clones were stained for alkaline phosphatase (AP) and counted. As expected, overexpression of Nanog in EF4 cells increased reprogramming. In contrast, AP+ and GFP+ colonies were strongly reduced by Dkk1 pretreatment of EF4 cells (Figures 2B, 2C, and S2A). Of note, cell-fusion efficiency was not modulated by Nanog overexpression or Dkk1 treatment (Figure S2B). These data indicated that activation of the Wnt pathway is essential for enhancement of reprogramming by Nanog.

These results were confirmed by the silencing of Dkk1 in wild-type ESCs (E14Tg2a) with a small hairpin (ShRNA) (Figures S2C–S2E), which induced stabilization of β-catenin (Figure S2D), increased levels of Axin2, and no changes in Nanog expression (Figure S2E); AP+ and GFP+ colonies were increased in ShRNA-Dkk1-E14Tg2a fused with NPCs-Oct4-Puro-GFP (Figures S2F–S2H).

Next, we generated ΔN4 and N1 clones after overexpressing Nanog in ESCs deleted for β-catenin (Δ/Δ) and in the parental wild-type cell line (fl/fl) (Lyashenko et al., 2011). These lines carried Nanog expression levels comparable to those in EF4 cells (Figure S2I), while Axin2, Cdx1, and Brachyury were overexpressed in N1, but not in ΔN4 cells (Figure S2J).

There was no increase in AP+ and GFP+ clones after fusion of ΔN4 cells with NPCs-Oct4-Puro-GFP, while there was increased reprogramming after fusion of N1 cells, with respect to controls (Figures 2D, 2E, and S2K). These data show that β-catenin is essential in the reprogramming process mediated by Nanog.

We ruled out reprogramming defects due to loss of stem features or cell-fusion capability of β-catenin null cells. Indeed, in serum+LIF medium, β-catenin null and the parental line had similar morphology (Figure S2L) and expressed normal levels of pluripotency genes (Figures S2M and S2N, fl/fl, Δ/Δ; Lyashenko et al., 2011). Furthermore, β-catenin null cells had no cell-adhesion defects, as shown by normal E-cadherin levels, which was probably due to upregulation of Plakoglobin and unchanged fusion efficiency (Figures S2N–S2P, fl/fl, Δ/Δ; Lyashenko et al., 2011). Similar features were also confirmed in another β-catenin null ESC line (Wray et al., 2011) (Figures S2N and S2O, fl/−, Δ/−; Wray et al., 2011).

Esrrb cooperates with Nanog in enhancement of reprogramming (Festuccia et al., 2012; Martello et al., 2012). We observed no changes in the expression of Esrrb, thereby excluding its role in reprogramming when Wnt/β-catenin activity was perturbed (Figure S2Q).

Finally, we also noted that Wnt3a levels were slightly higher in EF4 cells as compared to ΔN4 cells (Figure S2R); however,

(H) Dkk1 qPCR in EF4, wild-type ESCs (E14Tg2a, RF8), and Nanog βgeo/+.
(I) Western blot of Dkk1 in wild-type and mutant ESCs.
(J) Secreted Dkk1 concentration measured by ELISA assay.
Data are means ± SEM (n = 3). $p > 0.1$, $^{*}p < 0.05$, $^{**}p < 0.01$.

Please cite this article in press as: Marucci et al., β-Catenin Fluctuates in Mouse ESCs and Is Essential for Nanog-Mediated Reprogramming of Somatic Cells to Pluripotency, Cell Reports (2014), http://dx.doi.org/10.1016/j.celrep.2014.08.011

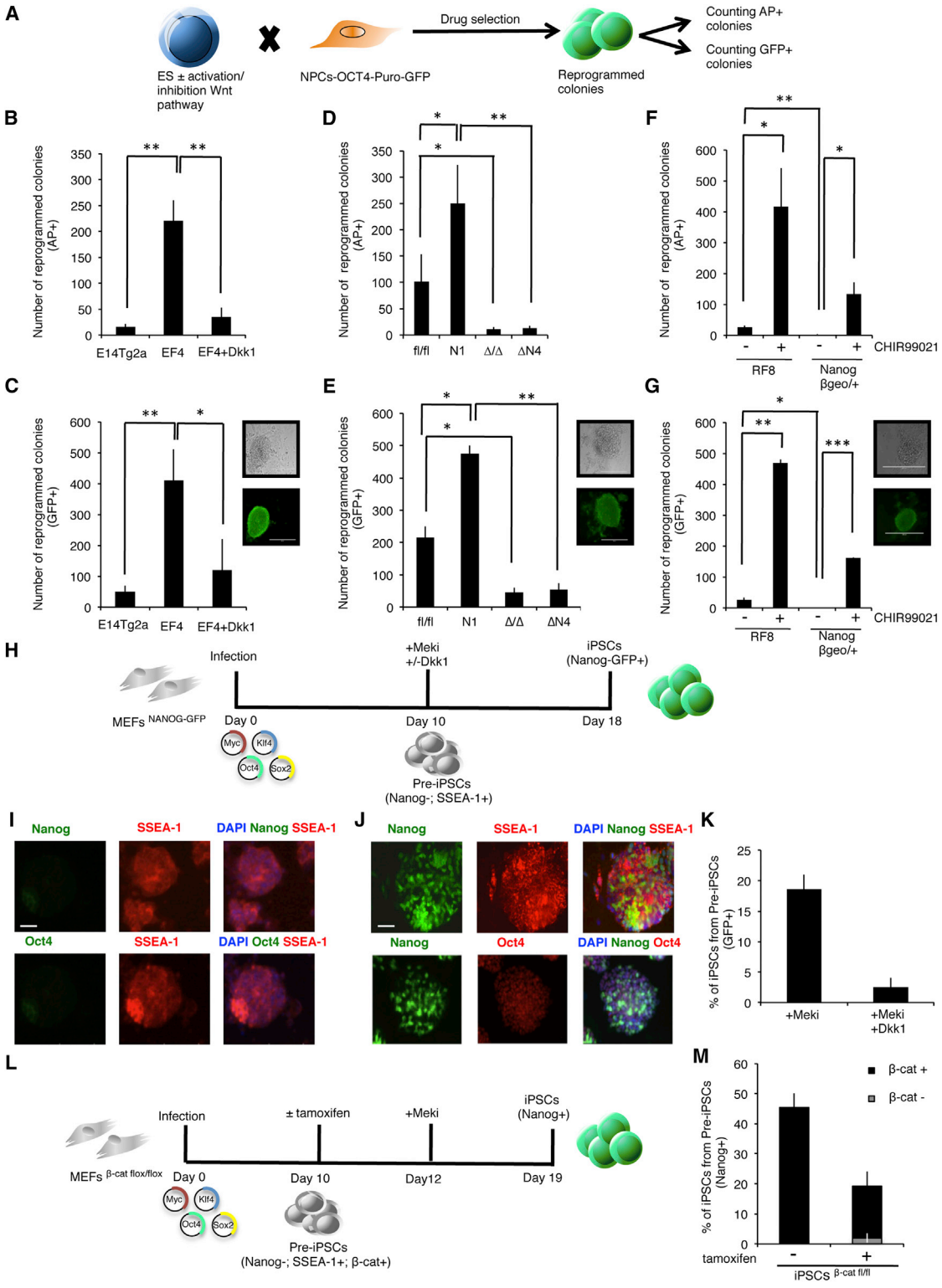


Figure 2. β-Catenin Is Essential for Nanog-Mediated Reprogramming of NPCs after Cell Fusion and for Conversion of Pre-iPSCs in iPSCs

(A) Scheme of spontaneous cell fusion between mESCs and NPCs.

(B and C) Reprogramming efficiency of E14Tg2a, EF4, and EF4 cells pretreated with Dkk1 (50 ng/ml, 24 hr), counting AP+ (B) and GFP+ (C) colonies. (C, inset) Representative GFP clone.

(legend continued on next page)

Chiron treatment induced upregulation of Wnt3a to similar levels in wild-type and βgeo/+ ESCs over the controls (Figure S2S). These data therefore excluded that overexpression of Nanog induces an upregulation of Wnt3a, which is dependent on β-catenin instead.

To further investigate β-catenin and Nanog interplay in reprogramming, we asked whether ESCs deleted for Nanog in one allele (Nanog βgeo/+) might not reprogram somatic cells after fusion, due to low β-catenin accumulation. Thus, we treated Nanog βgeo/+ and RF8 cells with Chiron, to stabilize β-catenin and activate target genes, without altering the levels of Nanog (Figures S2T and S2U), and fused these cells with NPCs-Oct4-Puro-GFP. No reprogrammed clones were selected after fusion of Nanog βgeo/+ ESCs, while reprogramming was greatly increased after fusion of Nanog βgeo/+ ESCs pretreated with Chiron (Figures 2F, 2G, and S2V). These data demonstrate that β-catenin stabilization with Chiron can rescue the lack of reprogramming after fusion of Nanog βgeo/+ ESCs.

Of note, Nanog βgeo/+ cells do not show pluripotency defects (Mitsui et al., 2003). Furthermore, E-cadherin and Plakoglobin levels and fusion efficiency were comparable to the parental line (Figures S2W–S2Y). Finally, reprogramming efficiency was not rescued by Wnt3a pretreatment of Nanog βgeo/+ ESCs (Figures S2Z–S2B^{I}). The low Nanog levels and consequently high Dkk1 in this cell line (Figure 1I) likely impaired the binding of Wnt3a to its receptor, as shown also by the lack of Wnt pathway activity (Figure S2C^{I}).

β-Catenin Is Essential for Nanog-Mediated Conversion of Pre-iPSCs into iPSCs

Stepwise modulation of the Wnt pathway is necessary for reprogramming mouse embryonic fibroblasts (MEFs) into iPSCs (Aulicino et al., 2014; Ho et al., 2013). Furthermore, Nanog is necessary for pre-iPSCs to become iPSCs (Silva et al., 2009). However, whether the Wnt pathway and Nanog cooperate in this conversion has not been studied.

MEFs stably carrying a GFP reporter for Nanog were infected with the mouse transcription factors Oct4, Klf4, Sox2, and c-Myc (OKSM) (Figure 2H). In pre-iPSCs positive for SSEA-1 and negative for Nanog (Figure S2D^{I}), we upregulated Nanog using a Mek inhibitor (Silva et al., 2008), and at the same time, we inhibited the Wnt pathway by adding Dkk1 (Figures 2H and S2E^{I}). There was a significantly reduced number of iPSCs generated from pre-iPSCs, while iPSCs were efficiently generated without inhibition of the Wnt pathway (Figures 2I–2K and S2F^{I}–S2H^{I}). We then further showed that inhibition of the Wnt pathway impairs the activity of Nanog in the late phase of reprogramming, as although Nanog was overexpressed in pre-iPSCs, the addition of Dkk1 drastically decreased iPSC number (Figures S2I^{I}–S2K^{I}).

Next, we investigated whether deletion of β-catenin in pre-iPSCs impairs their conversion into iPSCs. MEFs$^{\beta\text{-cat fl/fl}}$ were infected with OKSM (Figure 2L). The β-catenin gene was deleted in pre-iPSC colonies positive for SSEA-1 and negative for Nanog (Figures S2L^{I} and S2M^{I}). The deletion was not complete, however. After induction of Nanog with Mek inhibitor, pre-iPSCs$^{\beta\text{-cat }-/-}$ failed to become iPSCs, and there were no clones positive for Nanog and negative for β-catenin (Figures 2M and S2N^{I}). The few Nanog-positive clones selected (Figure 2M) were also positive for β-catenin, which indicated that they derived from MEFs that escaped β-catenin deletion. These were indistinguishable from iPSCs generated from pre-iPSCs$^{\beta\text{-cat fl/fl}}$ (Figures 2M and S2O^{I}). These data demonstrate that β-catenin is essential in the conversion of pre-iPSCs into iPSCs in establishing Nanog-mediated ground-state pluripotency.

β-Catenin Fluctuates Synchronously with Nanog in Serum+LIF Medium

Nanog fluctuates in ESCs cultured in serum+LIF medium (Chambers et al., 2007; MacArthur et al., 2012). We therefore investigated whether, apart from controlling reprogramming of somatic cells, the above-described Nanog regulation of Dkk1 affects β-catenin distribution and dynamics in ESCs.

In immunofluorescence experiments, there were heterogeneous levels of total and active β-catenin in E14Tg2a cultured in serum+LIF, with active β-catenin localized also in the nucleus, as expected (Figure 3A). Single cells expressing more Nanog also expressed high total and active β-catenin (Figure 3A), with high correlation (r = 0.78; Figure 3A). β-catenin-GFP was also heterogeneously expressed in EL55 cells, with these expressing high levels of β-catenin and Nanog, or low levels of both, as indicated by the correlation plot (r = 0.76; Figure 3B). Overall, these data indicate correlated heterogeneity of β-catenin and Nanog in ESCs cultured in serum+LIF.

We next investigated the dynamics of β-catenin in population studies and with time-lapse single-cell imaging. EL55 cultured in serum+LIF showed 45% ± 10% of GFP-positive cells, 15% ± 10% of GFP-negative cells, and a population with intermediate GFP levels (Figure 3C, Hβ-cat, Lβ-cat). Sorted Hβ-cat (GFP+) had higher levels of both β-catenin and Nanog with respect to

(D and E) Reprogramming efficiency comparing Nanog overexpression in β-catenin Δ/Δ background (ΔN4) and in β-catenin fl/fl background (N1), counting AP+ (D) and GFP+ (E) colonies. (E, inset) Representative GFP clone.

(F and G) Reprogramming efficiency stabilizing β-catenin with Chiron (3 μM, 24 hr) in βgeo/+ cells, counting AP+ (F) and GFP+ (G) colonies. (G, inset) Representative GFP clone.

(H) Scheme of iPSC generation. MEFs$^{\text{Nanog-GFP}}$ were infected with OKSM. Nanog-negative pre-iPSCs were cultured in ESC medium with the Mek inhibitor PD0325901 (Meki, 1 μM) ± Dkk1 (50 ng/ml).

(I and J) Immunofluorescence of pre-iPSCs grown in ESC medium containing Meki and Dkk1 (I) and of pre-iPSCs grown in ESC medium plus Meki (without Dkk1), converted into iPSCs (J).

(K) Percentage of Nanog-GFP+ iPSCs over total pre-iPSC clones.

(L) Scheme of iPSC generation from MEFs$^{\beta\text{-cat flox/flox}}$ after infection with OKSM. β-catenin was deleted in Nanog-negative pre-iPSCs with tamoxifen (1 μM). Pre-iPSCs ±tamoxifen were cultured in ESC medium with Meki to stabilize Nanog.

(M) Percentages of Nanog+ iPSCs over total pre-iPSC clones.

Data are means ± SEM (n = 5). $p > 0.1$, $^{*}p < 0.05$, $^{**}p < 0.01$, $^{***}p < 0.0001$. Scale bars represennt 200 μm (C, E, and G inset) and 25 μm (I and J).

OPEN ACCESS
CellPress

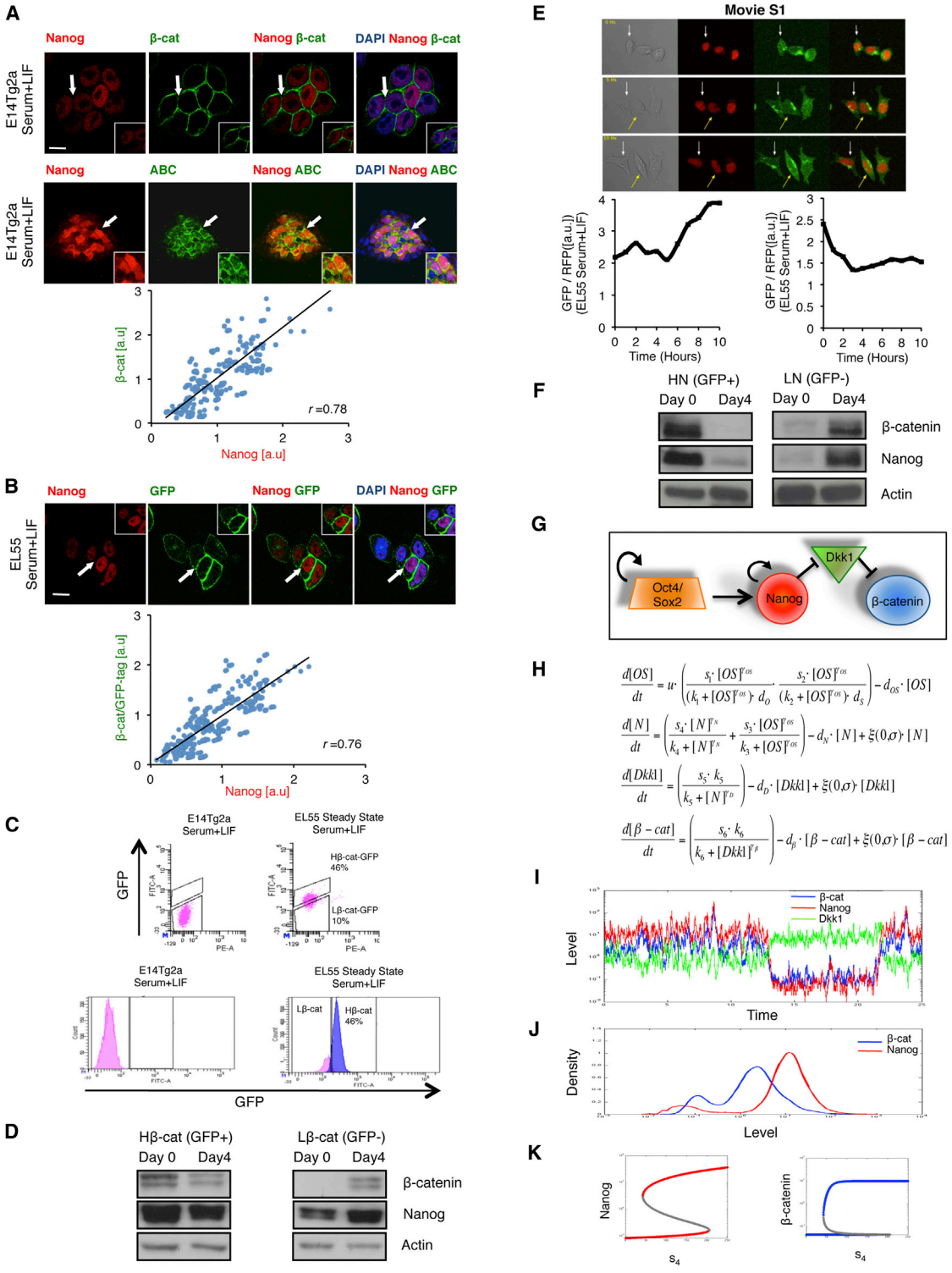


Figure 3. Correlated Fluctuations of β-Catenin and Nanog in ESCs Cultured in Serum+LIF Medium

(A and B) Immunofluorescences of total β-catenin, active β-catenin (ABC) and Nanog in E14Tg2a and EL55 cells cultured in serum+LIF. Arrows indicate zoomed regions with correlated expression of β-catenin and Nanog. The correlation plots of endogenous (A) and GFP-tagged (B) β-catenin with Nanog are shown (*r*, Pearson correlation coefficient).

(C) GFP distribution of the EL55 clone in serum+LIF analyzed by FACS. Hβ-cat, high β-catenin; Lβ-cat, low β-catenin.

(D) Western blot of GFP-positive (Hβ-cat) and GFP-negative (Lβ-cat) EL55 cells from FACS sorting (day 0) and 4 days of culture (day 4).

(legend continued on next page)

sorted Lβ-cat (GFP−) cells (Figure 3D, day 0). Levels of pluripotency genes were comparable (Figures S3A and S3B).

Next, we asked whether β-catenin spontaneously fluctuates over time, as had already been reported for Nanog. Hβ-cat (GFP+) and Lβ-cat (GFP–) fluorescence-activated cell sorting (FACS)-sorted cells passed from both Nanog and β-catenin "high states" to "low states" and vice versa, after 4 days of culture (Figure 3D).

We then analyzed β-catenin fluctuations using time-lapse single-cell imaging. The GFP signal was normalized against stably expressed red fluorescent protein fused to histone H2B (H2B-RFP). Unsynchronized EL55 cells cultured in serum+LIF showed increases and decreases in GFP levels over time (Movie S1; Figures 3E and S3C).

Finally, we showed correlated dynamics of Nanog and β-catenin in TNGA cells. FACS-sorted GFP+ (HN) had high levels of β-catenin, while GFP− (LN) cells had almost no β-catenin accumulation (Figure 3F, day 0). GFP+ cells had decreased levels of both β-catenin and Nanog at day 4. Symmetrical dynamics were observed in the GFP− population (Figure 3F). These data indicate that the levels of β-catenin and Nanog are dynamically interconnected in ESCs cultured in serum+LIF.

A Mathematical Model Recapitulates Nanog- and β-Catenin-Correlated Fluctuations

Different models have been proposed to explain Nanog dynamics (Fidalgo et al., 2012; Glauche et al., 2010; Kalmar et al., 2009; Navarro et al., 2012). To recapitulate the two different substates of Nanog and β-catenin in serum+LIF, we modeled the system as a bistable one, in which the low and high states of Nanog, and consequently of β-catenin, are both stable and the transition from one to the other is due to noise. Of note, gene expression noise is a major determinant of the distribution of Nanog in stem cells (Wu and Tzanakakis, 2012).

Oct4, Sox2, Nanog, Dkk1, and β-catenin interactions are considered in our model. The topology encompasses a positive autofeedback loop of Oct4-Sox2 heterodimer (Glauche et al., 2010), which activates Nanog expression (Rodda et al., 2005), and a positive autofeedback loop of Nanog (Loh et al., 2006; Mullin et al., 2008) (Figures 3G and S3D). Nanog has also been suggested to fluctuate because of autorepression (Fidalgo et al., 2012; Navarro et al., 2012). Here, we described the system using a minimal topology that encompasses bistability, as we mainly focused on the effects of Nanog fluctuations on β-catenin through Dkk1 repression, rather than on the regulation that controls the dynamics of Nanog.

We used first-order degradation kinetics and Hill functions for the transcriptional interactions. The model includes stochastic terms, implemented as zero-mean Gaussian processes, which are added to the equations for Nanog and β-catenin (Figure 3H). Starting from parameter values reported before (Abranches et al., 2013; Glauche et al., 2010), we measured the half-life of β-catenin (Figures S3E and S3F; Table S1) and modified the transcription rates and the amplitude of noise to fit the distribution of Nanog and β-catenin in TNGA and EL55 cells, respectively.

When simulating over time, a typical trajectory of Nanog, Dkk1, and β-catenin is presented (Figure 3I); due to noise, in serum+LIF, cells can switch from one steady state to the other, with correlated Nanog and β-catenin dynamics in antiphase with the Dkk1 ones. Simulating the model for a high number of cells and estimating the Kelner density (Cao et al., 1994), we recapitulated the stationary GFP distribution of TNGA and EL55 cells (Figures 1E, 1F, steady-state conditions, and Figure 3J). We captured the distributions observed in the two cell lines and the distances between the positive and negative states. Figure 3K shows typical bistability continuation plots; continuing the steady state on s_4 (the maximal rate of the autofeedback of Nanog), two saddle-node bifurcations delimit the bistability region.

β-Catenin Protein Is Heterogeneous in ESCs Cultured in 2i+LIF Medium

Recent reports have shown that Nanog and other members of the pluripotency network do not fluctuate when ESCs are cultured in 2i+LIF medium (Ying et al., 2008). We therefore asked whether β-catenin heterogeneity is also abrogated in ESCs cultured in 2i+LIF.

Nanog was overall homogeneously expressed in E14Tg2a cells, and instead, β-catenin was heterogeneous, with some cells accumulating more β-catenin in the nucleus and in the membranes than other cells in the same clone (Figure 4A). Furthermore, the correlation between Nanog and β-catenin levels was much lower in ESCs cultured in 2i+LIF (r = 0.51), as compared to serum+LIF (r = 0. 78) (Figures 3A and 4A). In EL55 cells cultured in 2i+LIF, although β-catenin-GFP fully colocalized with endogenous β-catenin with correlated expression (r = 0.98; Figure S4A), it was heterogeneously expressed, poorly correlating with Nanog (r = 0.56; Figure 4B).

Single-cell time lapses of EL55 cells cultured in 2i+LIF showed increases or decreases of GFP levels over time (Movies S2 and S3; Figures 4C, S4B, and S4C), which clearly demonstrated that β-catenin can fluctuate in ESCs in 2i+LIF.

In addition, we studied the dynamics of the pathway activity using TOP-dGFP, a well-known Wnt reporter carrying destabilized GFP (Biechele and Moon, 2008). Only 8% ± 5% of cells were GFP+ in 2i+LIF medium (Figure 4D). Furthermore, after plating the unsorted cells, we observed a variable number of GFP+ cells over time (Figures 4E and S4D), which confirmed the heterogeneous activity of the Wnt/β-catenin pathway. In addition,

(E) Snapshots of live EL55 cell imaging. Quantifications of GFP signal normalized against RFP signal, plotted as a function of time. White arrows, GFP switch off; yellow arrows, GFP switch on.
(F) HN (GFP+) and LN (GFP−) cells FACS sorted from TNGA ESCs and analyzed by western blot. HN, high Nanog; LN, low Nanog.
(G) Topology of the interactions among the Oct4-Sox2 heterodimer, Nanog, Dkk1, and β-catenin.
(H) Differential equations (DEs) model of the network.
(I) Nanog, Dkk1, and β-catenin simulated time course.
(J) Bimodal distribution of Nanog and β-catenin.
(K) Bifurcation plots of the model; red and blue lines indicate stable, while gray lines indicate unstable steady state. Scale bar represents 25 μm.

Please cite this article in press as: Marucci et al., β-Catenin Fluctuates in Mouse ESCs and Is Essential for Nanog-Mediated Reprogramming of Somatic Cells to Pluripotency, Cell Reports (2014), http://dx.doi.org/10.1016/j.celrep.2014.08.011

OPEN ACCESS
CellPress

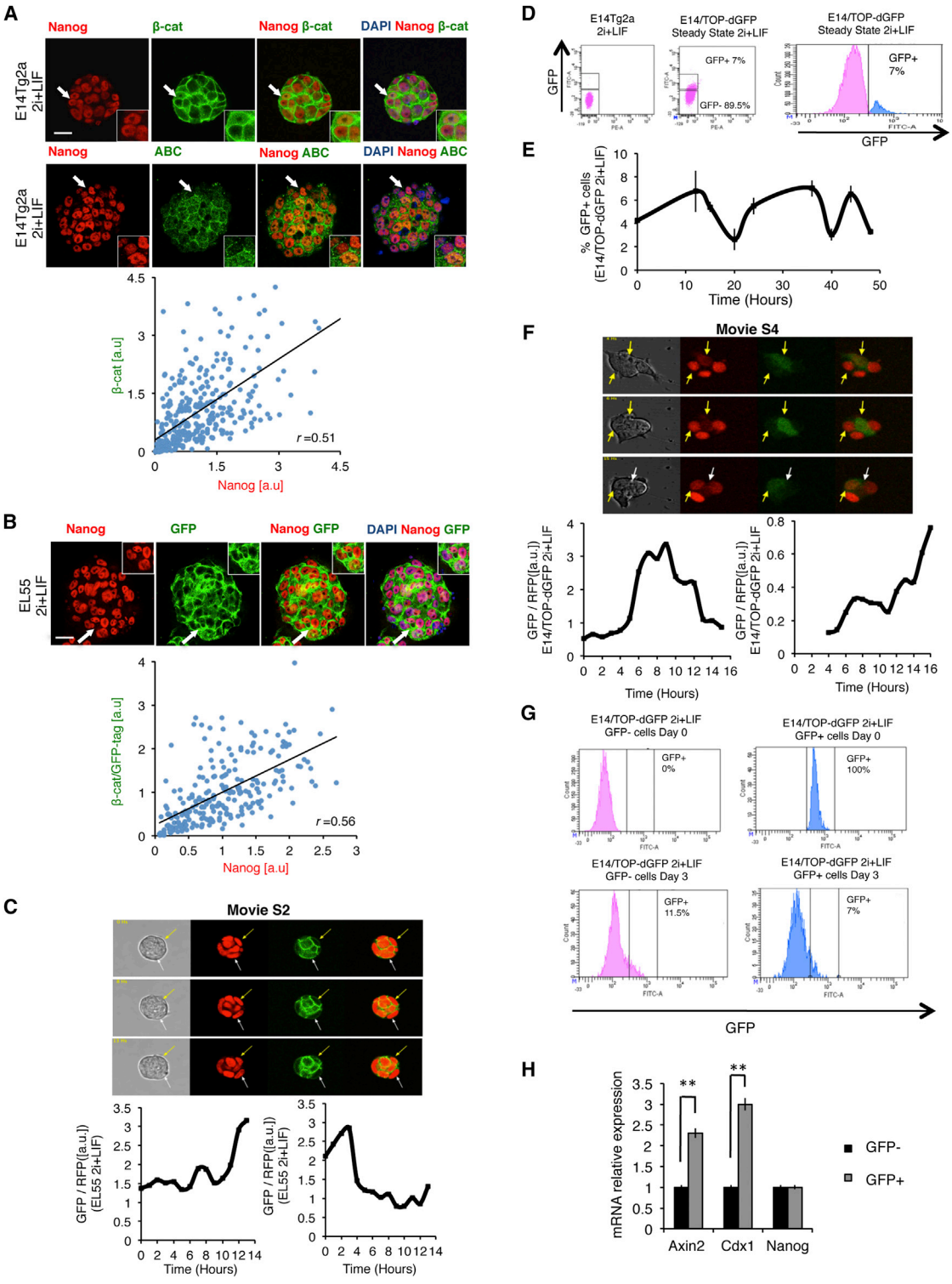


Figure 4. Dynamics of β-Catenin in Mouse ESCs Cultured in 2i+LIF Medium

(A and B) Immunofluorescences of β-catenin, active β-catenin (ABC), and Nanog in wild-type ESCs (E14Tg2a) and EL55 cells cultured in 2i+LIF. Arrows indicate zoomed regions with both correlated and uncorrelated expression of β-catenin and Nanog. The correlation plots of endogenous (A) and GFP-tagged (B) β-catenin with Nanog are shown (*r*, Pearson correlation coefficient).

(C) Snapshots of live EL55 cells imaged in 2i+LIF. Quantification of GFP normalized against RFP signal is plotted. White arrows, GFP switch off; yellow arrows, GFP switch on.

(legend continued on next page)

time-lapse single-cell imaging of E14/TOP-dGFP showed switching on and off of the reporter over time, as well as fluctuations between the two states (Movie S4; Figures 4F and S4E).

Finally, the TOP-dGFP reporter was activated 3 days after culturing FACS-sorted GFP− population in 2i+LIF, while it was inactivated in sorted GFP+ cells (Figure 4G). Target genes were active only in the sorted GFP+ cells, while Nanog did not change in both populations (Figure 4H).

Overall, these data indicate that β-catenin and its target genes can fluctuate in ground pluripotency state.

DISCUSSION

Crosstalk between the Wnt/β-catenin pathway and Nanog is important for ESC physiology. Here, we show that Nanog represses an important negative regulator of the Wnt pathway, Dkk1, and in turn indirectly activates β-catenin. This is essential for the function of Nanog during somatic cell reprogramming. On the other hand, we cannot exclude additional regulation by Nanog of other effectors of the pathway or that repression of Dkk1 by Nanog is in cooperation with a recruited repressor complex. Impairment of reprogramming due to lack of Nanog can be rescued by β-catenin stabilization, which implies a key function of β-catenin as a downstream effector of Nanog. Interestingly, there have been similar findings for Esrrb (Festuccia et al., 2012; Martello et al., 2012) and Tet1 and Tet2 (Costa et al., 2013), which are also Nanog-dependent factors in the establishment of pluripotency and reprogramming.

The regulation of Nanog on β-catenin in the reprogramming process is relevant regardless of transcriptional (Nusse, 2008; ten Berge et al., 2011) and nontranscriptional activities of β-catenin (Faunes et al., 2013), which might be synergistic, and therefore may be both important in the control of ESC pluripotency.

We used β-catenin null ESCs and confirmed published data (Lyashenko et al., 2011; Wray et al., 2011) that in the presence of LIF, these cells maintain pluripotency. Other studies have reported that removal of β-catenin affects pluripotency (Faunes et al., 2013). These divergences are probably due to the different strategies used to generate the lines.

Nanog is heterogeneous in serum+LIF, but only under feeder-free conditions, while it is homogeneous in 2i+LIF medium (Cahan and Daley, 2013; Smith, 2013), although some variability is expected (Faddah et al., 2013). Nanog dynamics were modeled as a single, stable, and high steady state, from which ESCs can escape due to intrinsic noise toward a transient state with low Nanog expression, in an excitable fashion (Kalmar et al., 2009). High and low Nanog states were also shown equally probable, and the dynamics of the transition between these as monotonic (Abranches et al., 2013). Here, we included Dkk1 and β-catenin and demonstrated that Nanog and β-catenin fluctuate synchronously with bistable dynamics due to stochastic noise.

Interestingly, in 2i+LIF medium, β-catenin fluctuates independently of Nanog. Fluctuations are probably regulated by negative feedback loops that result in Wnt pathway activation (Lee et al., 2003), as the 2i medium contains Chiron.

Nanog-dependent fluctuations are stochastic and are due to transcriptional noise; they might be important to prime cells toward differentiation. Upon Wnt pathway activation, fluctuating dynamics of β-catenin are not stochastic, as they can be controlled by negative feedback loops induced by drug treatments. Whether controlled β-catenin dynamics can maintain the ground state of ESC pluripotency remains an open question.

EXPERIMENTAL PROCEDURES

Cell Hybrids

For ESC and neural precursor cell (NPC) cocultures, 1.0×10^6 ESCs were plated onto preplated 1.0×10^6 NPCs. These were cocultured for 4 hr, first for 2 hr in NPC medium and then for 2 hr in ESC medium. The cells were then trypsinized and plated at 1/5 into p100 gelatin-coated dishes in ESC medium. After 72 hr, puromycin or hygromycin were added to the ESC medium for hybrid selection.

Time-Lapse Live Fluorescence Imaging

Images were acquired with a 40× (numerical aperture 0.55) lens using 488 nm and 561 nm excitation. A pinhole size of ~3 Airy units was used to increase signal. Cells were imaged at 37°C in a humidified environmental chamber in 5% CO_2. A time interval of 1 hr was set between time points. Image processing and fluorescence quantification were performed using ImageJ v1.47p.

Mathematical Model Simulation and Analysis

The stability and bifurcation analyses were realized using the software tool *xppaut* (http://www.math.pitt.edu/~bard/xpp/xpp.html). To approximate numerical solutions of the stochastic differential equations, we applied the Euler-Maruyama method. Stochastic simulations were implemented using the programming language C++. Density plots were generated under the MATLAB platform (MathWorks).

SUPPLEMENTAL INFORMATION

Supplemental information includes Supplemental Experimental Procedures, four figures, one table, and four movies and can be found with this article online at http://dx.doi.org/10.1016/j.celrep.2014.08.011.

AUTHOR CONTRIBUTIONS

M.P.C., L.M., and E.P. designed the experiments and data analysis. L.M., E.P., U.D.V., and B.S.E. performed experiments. M.I. designed the tagging strategy. L.M. developed the mathematical model. M.P.C., L.M., and E.P. wrote the manuscript. M.P.C. supervised the project.

ACKNOWLEDGMENTS

We thank K. Arumugam, F. Aulicino, A. Corsinotti, D. di Bernardo, J. Frade, F. Lluis, B. Keyes, L. Ombrato, and I. Theka for suggestions on the manuscript; B. Di Stefano for helping with pre-iPSC generation; M. Herberg for suggestions on the model; V. Chigancas, M. Muñoz, and N. Romo for technical support;

(D) GFP distribution in E14/TOP-dGFP by FACS. GFP+, high TOP-dGFP activity; GFP−, low TOP-dGFP activity.
(E) Time course of unsorted E14/TOP-dGFP grown in 2i+LIF and analyzed by FACS.
(F) Snapshots of live single E14/TOP-dGFP cell imaging and quantifications of GFP signal versus RFP. White arrows, GFP switch off; yellow arrows, GFP switch on.
(G) FACS analysis of GFP+ and GFP− cells sorted from E14/TOP-dGFP and cultured in 2i+LIF for 3 days.
(H) qPCR of Axin2, Cdx1, and Nanog in GFP+ and GFP− cells sorted from E14/TOP-dGFP cultured in 2i+LIF. Data are means ± SEM (n = 5). $^{**}p < 0.01$. Scale bar represents 25 μm.

Please cite this article in press as: Marucci et al., β-Catenin Fluctuates in Mouse ESCs and Is Essential for Nanog-Mediated Reprogramming of Somatic Cells to Pluripotency, Cell Reports (2014), http://dx.doi.org/10.1016/j.celrep.2014.08.011

A.M. Arias for suggestions on time-lapse imaging; and A. Smith, S. Yamanaka, I. Chambers, C. Hartmann, R. Farese, and B.E. Welm for cell lines and plasmids. This work was funded by an ERC grant (242630-RERE) (M.P.C.), an HFSP grant (M.P.C.), the Ministerio de Ciencia e Inovación SAF2011-28580 (M.P.C.), Fundacio La Marato de TV3 (M.P.C.), AXA Research Fund (M.P.C.), an EMBO Long-Term Fellowship (L.M.), and Wolfson Foundation and BBSRC Alert 13 capital grant (BB/L014181/1) (Bristol University).

Received: August 19, 2013
Revised: July 7, 2014
Accepted: August 6, 2014
Published: September 4, 2014

REFERENCES

Abranches, E., Bekman, E., and Henrique, D. (2013). Generation and characterization of a novel mouse embryonic stem cell line with a dynamic reporter of Nanog expression. PLoS ONE *8*, e59928.

Aulicino, F., Theka, I., Ombrato, L., Lluis, F., and Cosma, M.P. (2014). Temporal perturbation of the Wnt signaling pathway in the control of cell reprogramming is modulated by TCF1. Stem Cell Reports *2*, 707–720.

Biechele, T.L., and Moon, R.T. (2008). Assaying beta-catenin/TCF transcription with beta-catenin/TCF transcription-based reporter constructs. Methods Mol. Biol. *468*, 99–110.

Cahan, P., and Daley, G.Q. (2013). Origins and implications of pluripotent stem cell variability and heterogeneity. Nat. Rev. Mol. Cell Biol. *14*, 357–368.

Cao, R., Cuevas, A., and Manteiga, W.G. (1994). A comparative study of several smoothing methods in density estimation. Comput. Stat. Data Anal. *17*, 153–176.

Chambers, I., Colby, D., Robertson, M., Nichols, J., Lee, S., Tweedie, S., and Smith, A. (2003). Functional expression cloning of Nanog, a pluripotency sustaining factor in embryonic stem cells. Cell *113*, 643–655.

Chambers, I., Silva, J., Colby, D., Nichols, J., Nijmeijer, B., Robertson, M., Vrana, J., Jones, K., Grotewold, L., and Smith, A. (2007). Nanog safeguards pluripotency and mediates germline development. Nature *450*, 1230–1234.

Costa, Y., Ding, J., Theunissen, T.W., Faiola, F., Hore, T.A., Shliaha, P.V., Fidalgo, M., Saunders, A., Lawrence, M., Dietmann, S., et al. (2013). NANOG-dependent function of TET1 and TET2 in establishment of pluripotency. Nature *495*, 370–374.

Faddah, D.A., Wang, H., Cheng, A.W., Katz, Y., Buganim, Y., and Jaenisch, R. (2013). Single-cell analysis reveals that expression of nanog is biallelic and equally variable as that of other pluripotency factors in mouse ESCs. Cell Stem Cell *13*, 23–29.

Faunes, F., Hayward, P., Descalzo, S.M., Chatterjee, S.S., Balayo, T., Trott, J., Christoforou, A., Ferrer-Vaquer, A., Hadjantonakis, A.K., Dasgupta, R., and Arias, A.M. (2013). A membrane-associated β-catenin/Oct4 complex correlates with ground-state pluripotency in mouse embryonic stem cells. Development *140*, 1171–1183.

Festuccia, N., Osorno, R., Halbritter, F., Karwacki-Neisius, V., Navarro, P., Colby, D., Wong, F., Yates, A., Tomlinson, S.R., and Chambers, I. (2012). Esrrb is a direct Nanog target gene that can substitute for Nanog function in pluripotent cells. Cell Stem Cell *11*, 477–490.

Fidalgo, M., Faiola, F., Pereira, C.F., Ding, J., Saunders, A., Gingold, J., Schaniel, C., Lemischka, I.R., Silva, J.C., and Wang, J. (2012). Zfp281 mediates Nanog autorepression through recruitment of the NuRD complex and inhibits somatic cell reprogramming. Proc. Natl. Acad. Sci. USA *109*, 16202–16207.

Glauche, I., Herberg, M., and Roeder, I. (2010). Nanog variability and pluripotency regulation of embryonic stem cells—insights from a mathematical model analysis. PLoS ONE *5*, e11238.

Hayashi, K., Lopes, S.M., Tang, F., and Surani, M.A. (2008). Dynamic equilibrium and heterogeneity of mouse pluripotent stem cells with distinct functional and epigenetic states. Cell Stem Cell *3*, 391–401.

Ho, R., Papp, B., Hoffman, J.A., Merrill, B.J., and Plath, K. (2013). Stage-specific regulation of reprogramming to induced pluripotent stem cells by Wnt signaling and T cell factor proteins. Cell Reports *3*, 2113–2126.

Kalmar, T., Lim, C., Hayward, P., Muñoz-Descalzo, S., Nichols, J., Garcia-Ojalvo, J., and Martinez Arias, A. (2009). Regulated fluctuations in nanog expression mediate cell fate decisions in embryonic stem cells. PLoS Biol. *7*, e1000149.

Kawano, Y., and Kypta, R. (2003). Secreted antagonists of the Wnt signalling pathway. J. Cell Sci. *116*, 2627–2634.

Kotini, A.G., Mpakali, A., and Agalioti, T. (2011). Dnmt3a1 upregulates transcription of distinct genes and targets chromosomal gene clusters for epigenetic silencing in mouse embryonic stem cells. Mol. Cell. Biol. *31*, 1577–1592.

Kühl, S.J., and Kühl, M. (2013). On the role of Wnt/β-catenin signaling in stem cells. Biochim. Biophys. Acta *1830*, 2297–2306.

Lee, E., Salic, A., Krüger, R., Heinrich, R., and Kirschner, M.W. (2003). The roles of APC and Axin derived from experimental and theoretical analysis of the Wnt pathway. PLoS Biol. *1*, E10.

Lluis, F., and Cosma, M.P. (2009). Somatic cell reprogramming control: signaling pathway modulation versus transcription factor activities. Cell Cycle *8*, 1138–1144.

Lluis, F., Pedone, E., Pepe, S., and Cosma, M.P. (2008). Periodic activation of Wnt/beta-catenin signaling enhances somatic cell reprogramming mediated by cell fusion. Cell Stem Cell *3*, 493–507.

Lluis, F., Pedone, E., Pepe, S., and Cosma, M.P. (2010). The Wnt/β-catenin signaling pathway tips the balance between apoptosis and reprograming of cell fusion hybrids. Stem Cells *28*, 1940–1949.

Loh, Y.H., Wu, Q., Chew, J.L., Vega, V.B., Zhang, W., Chen, X., Bourque, G., George, J., Leong, B., Liu, J., et al. (2006). The Oct4 and Nanog transcription network regulates pluripotency in mouse embryonic stem cells. Nat. Genet. *38*, 431–440.

Lyashenko, N., Winter, M., Migliorini, D., Biechele, T., Moon, R.T., and Hartmann, C. (2011). Differential requirement for the dual functions of β-catenin in embryonic stem cell self-renewal and germ layer formation. Nat. Cell Biol. *13*, 753–761.

MacArthur, B.D., Sevilla, A., Lenz, M., Müller, F.J., Schuldt, B.M., Schuppert, A.A., Ridden, S.J., Stumpf, P.S., Fidalgo, M., Ma'ayan, A., et al. (2012). Nanog-dependent feedback loops regulate murine embryonic stem cell heterogeneity. Nat. Cell Biol. *14*, 1139–1147.

Marks, H., Kalkan, T., Menafra, R., Denissov, S., Jones, K., Hofemeister, H., Nichols, J., Kranz, A., Stewart, A.F., Smith, A., and Stunnenberg, H.G. (2012). The transcriptional and epigenomic foundations of ground state pluripotency. Cell *149*, 590–604.

Marson, A., Foreman, R., Chevalier, B., Bilodeau, S., Kahn, M., Young, R.A., and Jaenisch, R. (2008). Wnt signaling promotes reprogramming of somatic cells to pluripotency. Cell Stem Cell *3*, 132–135.

Martello, G., Sugimoto, T., Diamanti, E., Joshi, A., Hannah, R., Ohtsuka, S., Göttgens, B., Niwa, H., and Smith, A. (2012). Esrrb is a pivotal target of the Gsk3/Tcf3 axis regulating embryonic stem cell self-renewal. Cell Stem Cell *11*, 491–504.

Mitsui, K., Tokuzawa, Y., Itoh, H., Segawa, K., Murakami, M., Takahashi, K., Maruyama, M., Maeda, M., and Yamanaka, S. (2003). The homeoprotein Nanog is required for maintenance of pluripotency in mouse epiblast and ES cells. Cell *113*, 631–642.

Mullin, N.P., Yates, A., Rowe, A.J., Nijmeijer, B., Colby, D., Barlow, P.N., Walkinshaw, M.D., and Chambers, I. (2008). The pluripotency rheostat Nanog functions as a dimer. Biochem. J. *411*, 227–231.

Navarro, P., Festuccia, N., Colby, D., Gagliardi, A., Mullin, N.P., Zhang, W., Karwacki-Neisius, V., Osorno, R., Kelly, D., Robertson, M., and Chambers, I. (2012). OCT4/SOX2-independent Nanog autorepression modulates heterogeneous Nanog gene expression in mouse ES cells. EMBO J. *31*, 4547–4562.

Niehrs, C. (2006). Function and biological roles of the Dickkopf family of Wnt modulators. Oncogene *25*, 7469–7481.

Nusse, R. (2008). Wnt signaling and stem cell control. Cell Res. *18*, 523–527.

Rodda, D.J., Chew, J.L., Lim, L.H., Loh, Y.H., Wang, B., Ng, H.H., and Robson, P. (2005). Transcriptional regulation of nanog by OCT4 and SOX2. J. Biol. Chem. *280*, 24731–24737.

Sato, N., Meijer, L., Skaltsounis, L., Greengard, P., and Brivanlou, A.H. (2004). Maintenance of pluripotency in human and mouse embryonic stem cells through activation of Wnt signaling by a pharmacological GSK-3-specific inhibitor. Nat. Med. *10*, 55–63.

Silva, J., Chambers, I., Pollard, S., and Smith, A. (2006). Nanog promotes transfer of pluripotency after cell fusion. Nature *441*, 997–1001.

Silva, J., Barrandon, O., Nichols, J., Kawaguchi, J., Theunissen, T.W., and Smith, A. (2008). Promotion of reprogramming to ground state pluripotency by signal inhibition. PLoS Biol. *6*, e253.

Silva, J., Nichols, J., Theunissen, T.W., Guo, G., van Oosten, A.L., Barrandon, O., Wray, J., Yamanaka, S., Chambers, I., and Smith, A. (2009). Nanog is the gateway to the pluripotent ground state. Cell *138*, 722–737.

Smith, A. (2013). Nanog heterogeneity: tilting at windmills? Cell Stem Cell *13*, 6–7.

Sokol, S.Y. (2011). Maintaining embryonic stem cell pluripotency with Wnt signaling. Development *138*, 4341–4350.

Stamos, J.L., and Weis, W.I. (2013). The β-catenin destruction complex. Cold Spring Harb. Perspect. Biol. *5*, a007898.

ten Berge, D., Kurek, D., Blauwkamp, T., Koole, W., Maas, A., Eroglu, E., Siu, R.K., and Nusse, R. (2011). Embryonic stem cells require Wnt proteins to prevent differentiation to epiblast stem cells. Nat. Cell Biol. *13*, 1070–1075.

van den Berg, D.L., Zhang, W., Yates, A., Engelen, E., Takacs, K., Bezstarosti, K., Demmers, J., Chambers, I., and Poot, R.A. (2008). Estrogen-related receptor beta interacts with Oct4 to positively regulate Nanog gene expression. Mol. Cell. Biol. *28*, 5986–5995.

Wray, J., Kalkan, T., and Smith, A.G. (2010). The ground state of pluripotency. Biochem. Soc. Trans. *38*, 1027–1032.

Wray, J., Kalkan, T., Gomez-Lopez, S., Eckardt, D., Cook, A., Kemler, R., and Smith, A. (2011). Inhibition of glycogen synthase kinase-3 alleviates Tcf3 repression of the pluripotency network and increases embryonic stem cell resistance to differentiation. Nat. Cell Biol. *13*, 838–845.

Wu, J., and Tzanakakis, E.S. (2012). Contribution of stochastic partitioning at human embryonic stem cell division to NANOG heterogeneity. PLoS ONE *7*, e50715.

Ying, Q.L., Wray, J., Nichols, J., Batlle-Morera, L., Doble, B., Woodgett, J., Cohen, P., and Smith, A. (2008). The ground state of embryonic stem cell self-renewal. Nature *453*, 519–523.

Cell Reports, Volume *8*

Supplemental Information

β-Catenin Fluctuates in Mouse ESCs and Is Essential for Nanog-Mediated Reprogramming of Somatic Cells to Pluripotency

Lucia Marucci, Elisa Pedone, Umberto Di Vicino, Blanca Sanuy-Escribano, Mark Isalan, and Maria Pia Cosma

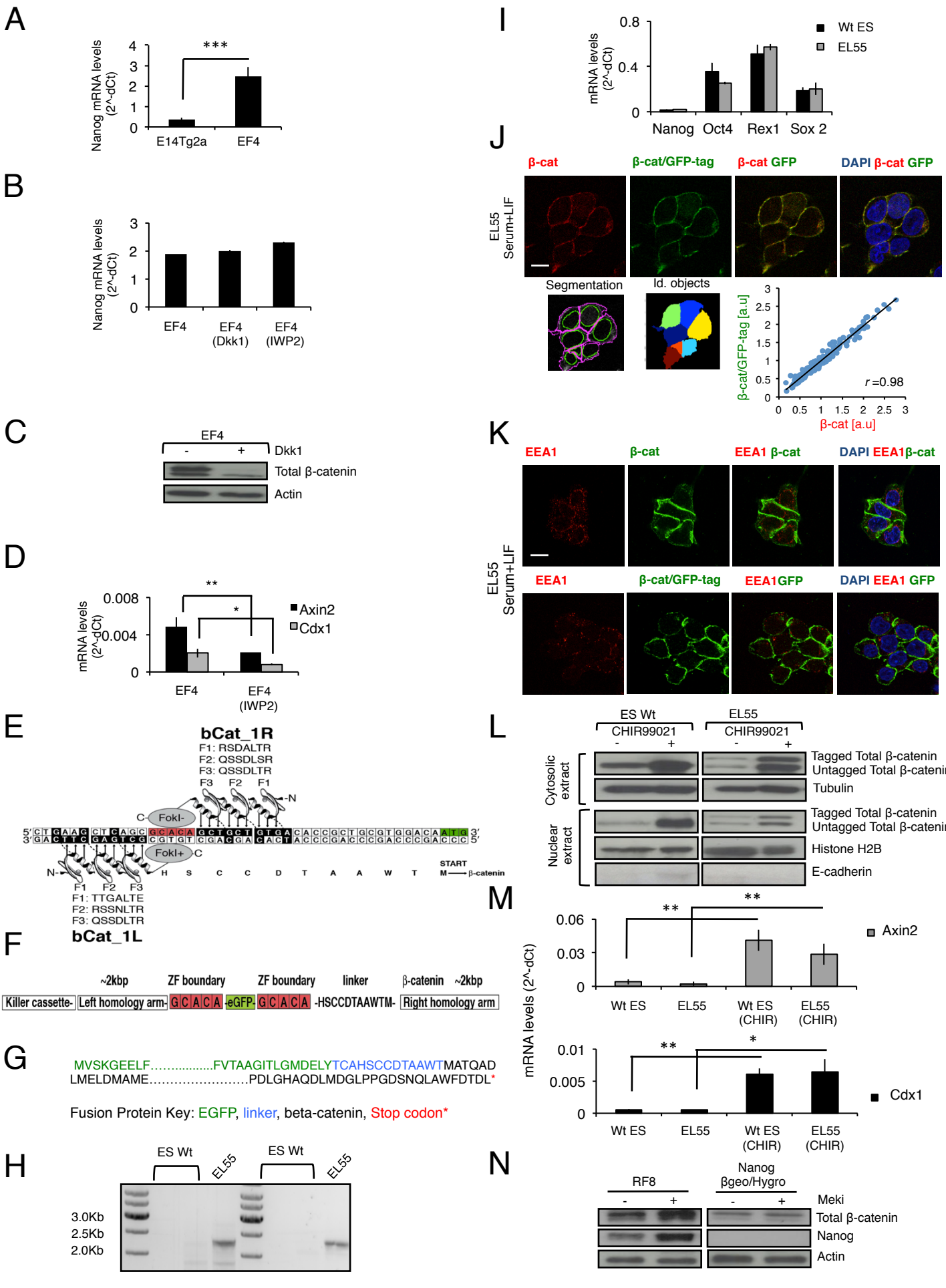
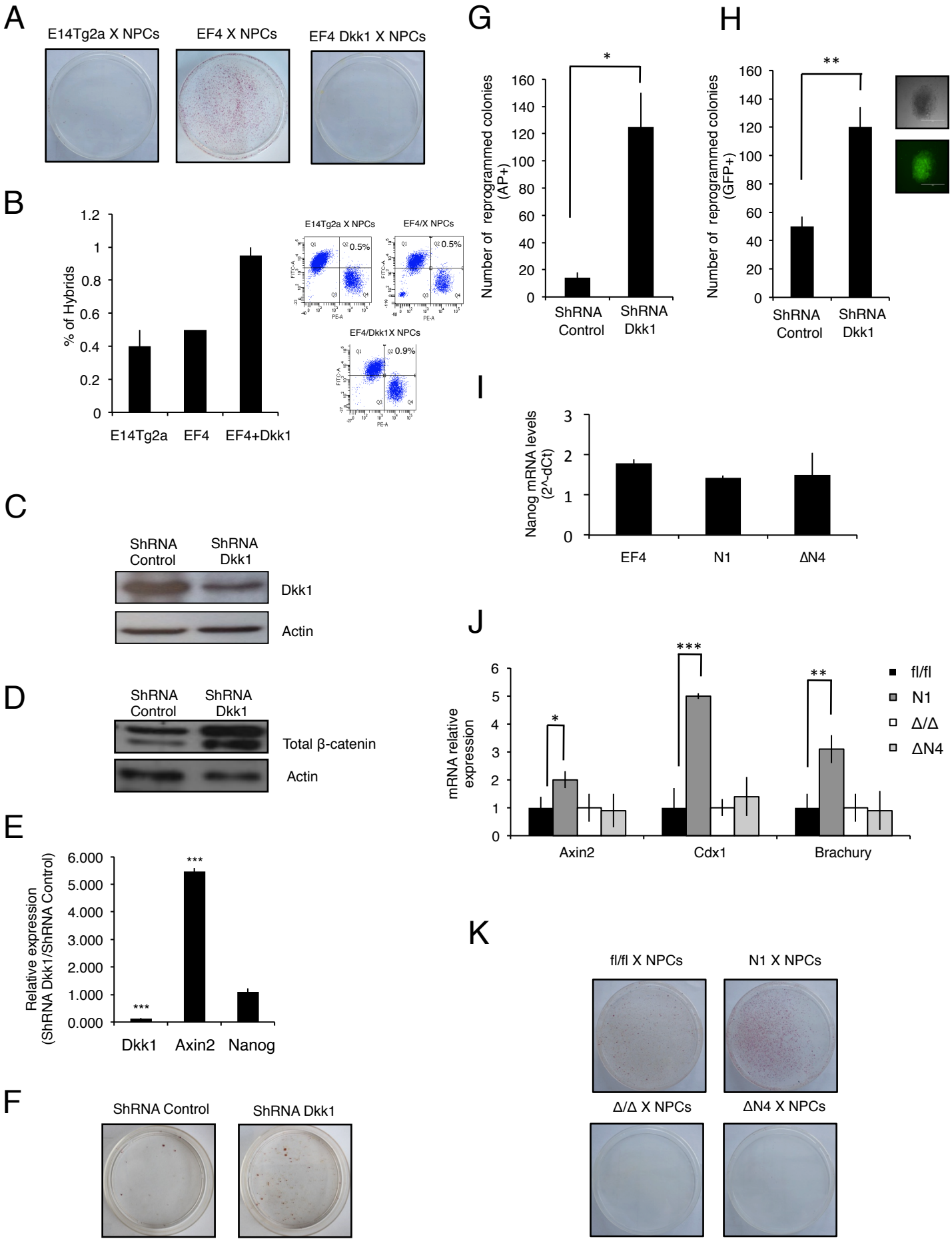
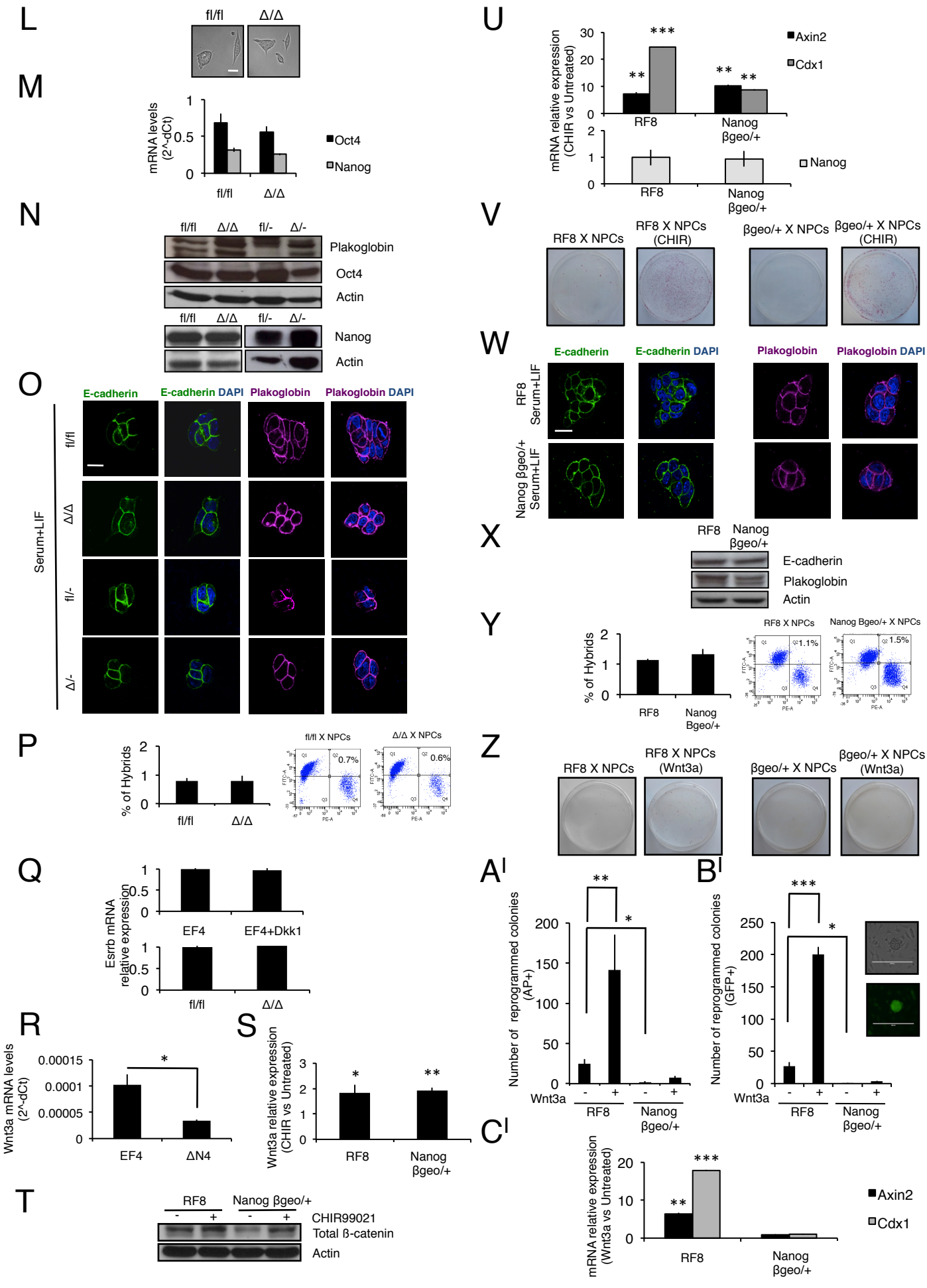

A
Nanog mRNA levels (2^-dCt)
***
E14Tg2a
EF4
B
Nanog mRNA levels (2^-dCt)
EF4
EF4 (Dkk1)
EF4 (IWP2)
C
EF4
Dkk1
Total β-catenin
Actin
D
mRNA levels (2^-dCt)
Axin2
Cdx1
EF4
EF4 (IWP2)
E
bCat_1R
F1: RSDALTR
F2: QSSDLSR
F3: QSSDLTR
FokI-
FokI+
START
bCat_1L
F1: TTGALTE
F2: RSSNLTR
F3: QSSDLTR
F
~2kbp
ZF boundary
ZF boundary
linker
β-catenin
~2kbp
Killer cassette-
Left homology arm-
-eGFP-
-HSCCDTAAWTM-
Right homology arm
G
MVSKGEELF.....FVTAAGITLGMDELYTCAHSCCDTAAWTMATQAD
LMELDMAME.....PDLGHAQDLMDGLPPGDSNQLAWFDTDL*
Fusion Protein Key: EGFP, linker, beta-catenin, Stop codon*
H
ES Wt
EL55
ES Wt
EL55
3.0Kb
2.5Kb
2.0Kb
I
mRNA levels (2^-dCt)
Wt ES
EL55
Nanog
Oct4
Rex1
Sox 2
J
β-cat
β-cat/GFP-tag
β-cat GFP
DAPI β-cat GFP
EL55 Serum+LIF
Segmentation
Id. objects
β-cat/GFP-tag [a.u]
β-cat [a.u]
r =0.98
K
EEA1
β-cat
EEA1 β-cat
DAPI EEA1β-cat
EEA1
β-cat/GFP-tag
EEA1GFP
DAPI EEA1 GFP
EL55 Serum+LIF
L
ES Wt
EL55
CHIR99021
Cytosolic extract
Nuclear extract
Tagged Total β-catenin
Untagged Total β-catenin
Tubulin
Histone H2B
E-cadherin
M
mRNA levels (2^-dCt)
Axin2
Cdx1
Wt ES
EL55
Wt ES (CHIR)
EL55 (CHIR)
N
RF8
Nanog βgeo/Hygro
Meki
Total β-catenin
Nanog
Actin

Figure S1. Tagging of β-catenin in mouse ESCs and mESCs characterization. Related to Figure 1.

(A) qPCR of Nanog expression in E14Tg2a and EF4 cells. (B) qPCR of Nanog mRNA in EF4 cells treated with Dkk1, with IWP2 or left untreated. (C) Western blot of total β-catenin in EF4 cells untreated or treated with recombinant Dkk1. (D) qPCR of the β-catenin target genes in EF4 cells untreated or treated with IWP2. (E) Schematic model showing designed zinc fingers aligned to their target DNA just upstream of the β-catenin start codon (ATG; green). Arrows indicate canonical base contacts. Zinc finger α-helix sequences that are involved in DNA recognition, are indicated (F1, Finger 1, etc.). The FokI moities are shown as positively (+) or negatively (-) charged to allow obligate heterodimer formation. The nuclease cutting region is in red. Part of the genomic DNA codes for a protein linker to β-catenin in the final eGFP fusion (HSCCDTAAWTM). (F) Donor DNA design indicating the homology arms that match the DNA between the donor plasmid and the genomic region. (G) Scheme of the GFP-β-catenin fusion protein. The tagging is at the N-terminus. (H) PCR amplification of the tagged allele using genomic DNA of EL55 cells. (I) qPCR of pluripotency genes in EL55 cells. (J) Immunofluorescence of total β-catenin and GFP in EL55 cells cultured in serum+LIF medium and correlation plot of β-catenin and GFP in EL55 cells (*r* is the Pearson correlation coefficient). Segmented images and identified objects are shown. (K) Co-immunofluorescence of GFP- β-catenin and endogenous β-catenin with EEA1 (early endosome) in EL55 cells cultured in serum+LIF medium. (L) Western blot of total β-catenin using cytosolic and nuclear extracts of EL55 cells after 1 day of CHIR99021 treatment (3 μM). E-cadherin is used as negative control for nuclear extracts. Tubulin and Histone H2B were used as housekeeping genes for cytosolic and nuclear extracts, respectively. (M) qPCR of Axin2 and Cdx1 upon CHIR99021 treatment. (N) Western blot of β-catenin and Nanog in wild-type ESCs (RF8 cells) and in Nanog-null cells (β geo/Hygro) untreated or treated for 1 week with Meki (PD184352; 3 μM). Data are

means ±SEM (n = 3). p >0.1, *, p <0.05, **, p <0.01, ***, p <0.0001. Scale bar, 25 μm.


A
E14Tg2a X NPCs
EF4 X NPCs
EF4 Dkk1 X NPCs
B
% of Hybrids
E14Tg2a
EF4
EF4+Dkk1
E14Tg2a X NPCs
EF4/X NPCs
EF4/Dkk1X NPCs
0.5%
0.5%
0.9%
C
ShRNA Control
ShRNA Dkk1
Dkk1
Actin
D
ShRNA Control
ShRNA Dkk1
Total β-catenin
Actin
E
Relative expression (ShRNA Dkk1/ShRNA Control)
Dkk1
Axin2
Nanog
F
ShRNA Control
ShRNA Dkk1
G
Number of reprogrammed colonies (AP+)
ShRNA Control
ShRNA Dkk1
H
Number of reprogrammed colonies (GFP+)
ShRNA Control
ShRNA Dkk1
I
Nanog mRNA levels (2^-dCt)
EF4
N1
ΔN4
J
mRNA relative expression
Axin2
Cdx1
Brachury
fl/fl
N1
Δ/Δ
ΔN4
K
fl/fl X NPCs
N1 X NPCs
Δ/Δ X NPCs
ΔN4 X NPCs


L
fl/fl
Δ/Δ
M
mRNA levels (2^-dCt)
Oct4
Nanog
N
fl/fl
Δ/Δ
fl/-
Δ/-
Plakoglobin
Oct4
Actin
Nanog
Actin
O
E-cadherin
E-cadherin DAPI
Plakoglobin
Plakoglobin DAPI
Serum+LIF
P
% of Hybrids
fl/fl X NPCs
Δ/Δ X NPCs
0.7%
0.6%
Q
Esrrb mRNA relative expression
EF4
EF4+Dkk1
R
Wnt3a mRNA levels (2^-dCt)
EF4
ΔN4
S
Wnt3a relative expression (CHIR vs Untreated)
RF8
Nanog βgeo/+
T
RF8
Nanog βgeo/+
CHIR99021
Total ß-catenin
Actin
U
mRNA relative expression (CHIR vs Untreated)
Axin2
Cdx1
Nanog
RF8
Nanog βgeo/+
V
RF8 X NPCs
RF8 X NPCs (CHIR)
βgeo/+ X NPCs
βgeo/+ X NPCs (CHIR)
W
E-cadherin
E-cadherin DAPI
Plakoglobin
Plakoglobin DAPI
RF8 Serum+LIF
Nanog βgeo/+ Serum+LIF
X
RF8
Nanog βgeo/+
E-cadherin
Plakoglobin
Actin
Y
% of Hybrids
RF8
Nanog Bgeo/+
RF8 X NPCs
Nanog Bgeo/+ X NPCs
1.1%
1.5%
Z
RF8 X NPCs
RF8 X NPCs (Wnt3a)
βgeo/+ X NPCs
βgeo/+ X NPCs (Wnt3a)
A^I
Number of reprogrammed colonies (AP+)
Wnt3a
RF8
Nanog βgeo/+
B^I
Number of reprogrammed colonies (GFP+)
Wnt3a
RF8
Nanog βgeo/+
C^I
mRNA relative expression (Wnt3a vs Untreated)
Axin2
Cdx1
RF8
Nanog βgeo/+

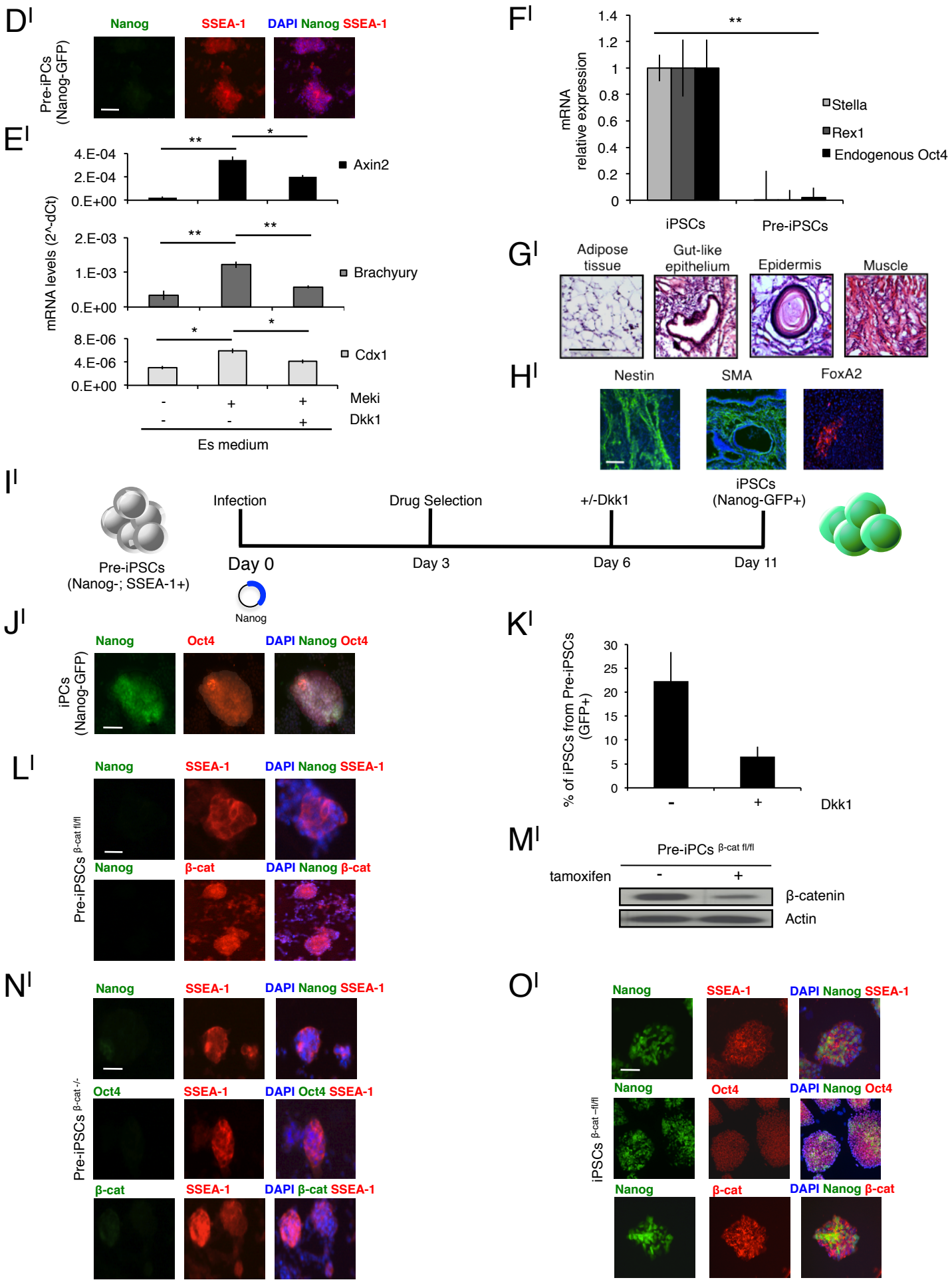

D
Nanog
SSEA-1
DAPI Nanog SSEA-1
Pre-iPCs (Nanog-GFP)
E
mRNA levels (2^-dCt)
Axin2
Brachyury
Cdx1
Meki
Dkk1
Es medium
F
mRNA relative expression
Stella
Rex1
Endogenous Oct4
iPSCs
Pre-iPSCs
G
Adipose tissue
Gut-like epithelium
Epidermis
Muscle
H
Nestin
SMA
FoxA2
I
Pre-iPSCs (Nanog-; SSEA-1+)
Infection
Drug Selection
+/-Dkk1
iPSCs (Nanog-GFP+)
Day 0
Day 3
Day 6
Day 11
Nanog
J
iPCs (Nanog-GFP)
Nanog
Oct4
DAPI Nanog Oct4
K
% of iPSCs from Pre-iPSCs (GFP+)
Dkk1
L
Pre-iPSCs β-cat fl/fl
Nanog
SSEA-1
DAPI Nanog SSEA-1
β-cat
DAPI Nanog β-cat
M
Pre-iPSCs β-cat fl/fl
tamoxifen
β-catenin
Actin
N
Pre-iPSCs β-cat -/-
Oct4
DAPI Oct4 SSEA-1
DAPI β-cat SSEA-1
O
iPSCs β-cat −fl/fl
DAPI Nanog Oct4
DAPI Nanog β-cat

Figure S2. Characterization of wild type and mutant mESCs and of reprogramming experiments, Related to Figure 2.

(A) Representative images of AP staining of clones obtained after spontaneous cell fusion between NPCs and E14Tg2a, EF4 and EF4 cells pretreated with Dkk1. (B) NPCs were co-cultured with E14Tg2a or with EF4 or with Dkk1-treated EF4 for 4 hours. The percentage of the hybrids was evaluated by FACS analysis. Representative FACS profiles of the hybrids are shown. (C) Western blot of Dkk1 after the infection of wild type E14Tg2a ESCs with ShRNA Control and ShRNA against Dkk1. (D) Western blot of total β-catenin after infection of E14Tg2a ESCs with ShRNA Control and ShRNA against Dkk1. (E) Dkk1, Axin2 and Nanog expression in ESCs infected with ShRNA against Dkk1. (F-H) Activation of the Wnt pathway by silencing Dkk1 increases the reprogramming efficiency. (F) Representative images of AP staining. (G and H) Quantification of reprogramming efficiency, counting AP+ (G) and GFP+ (H) colonies. (H, inset) Representative GFP clone. (I) qPCR of Nanog in Nanog overexpressing N1 (β-catenin fl/fl) and ΔN4 (β-catenin Δ/Δ) cell lines. (J) Expression of β-catenin target genes in N1 cells, ΔN4 cells and their parental lines. (K) Representative images of AP staining of clones obtained after spontaneous cell fusion between NPCs and β-catenin fl/fl, β-catenin Δ/Δ, ΔN4 and N1 ESCs. (L-P) Characterization of β-catenin null ESCs and their parental lines. (L) Bright field microphotograph of wild type β-catenin and β-catenin null ESCs. (M and N) qPCR and western blot of the pluripotency genes and Plakoglobin in wild type fl/fl β-catenin and Δ/Δ β-catenin ESCs (Lyashenko et al., 2011) as well as in wild type fl/- β-catenin and Δ/- β-catenin ESCs (Wray et al., 2011) cultured in serum+LIF medium. (O) Immunofluorescence of E-cadherin and Plakoglobin in wild type and β-catenin null ESCs as indicated in B and C cultured in serum+LIF medium. (P) Percentage of hybrids analyzed by FACS after 4h of co-culture of NPCs with β-catenin fl/fl or β-catenin Δ/Δ ESCs. Representative FACS profiles of the hybrids are shown. (Q) qPCR of Esrrb in EF4 ±Dkk1, β-catenin fl/fl and β-catenin Δ/Δ. (R) qPCR of Wnt3a expression in EF4 and ΔN4 cells. (S) qPCR of Wnt3a expression upon CHIR99021 treatment of RF8 and of Nanog β geo/+ cells (treated *vs* untreated).

(T) Western blot of total β-catenin in wild-type ESCs (RF8 cells) and in cells lacking one copy of Nanog (Nanog βgeo/+ cells) upon CHIR99021 treatment. (U) qPCR of β-catenin target genes and Nanog in RF8 and Nanog βgeo/+ cells upon the activation of the pathway with CHIR9902 (treated *vs* untreated). (V) Representative images of AP staining (spontaneous cell fusion between NPCs and RF8 or βgeo/+ ESCs untreated, or treated for 24 h with Chiron 3 μM). (W) Immunofluorescence of E-cadherin and Plakoglobin in RF8 and Nanog βgeo/+ cells cultured in serum+LIF medium. (X) Western blot of E-cadherin and Plakoglobin in RF8 and Nanog βgeo/+ cells cultured in serum+LIF medium. (Y) Percentage of hybrids analyzed by FACS after 4h of co-culture of NPCs with RF8 or Nanog βgeo/+ cells. Representative FACS profiles of the hybrids are shown. (Z-B^{I}) Stabilization of β-catenin levels using recombinant Wnt3a (48 h, 200ng/mL) does not rescue the reprogramming deficiency of cells lacking one copy of Nanog (βgeo/+). (Z) Representative images of AP staining. (A^{I} and B^{I}) Quantification of reprogramming efficiency, counting AP+ (A^{I}) and GFP+ (B^{I}) colonies. (B^{I}, inset) Representative GFP clone. (C^{I}) qPCR of the β-catenin target genes in RF8 and Nanog βgeo/+ cells upon the activation of the pathway with recombinant Wnt3a (treated *vs* untreated). (D^{I}) Immunofluorescence of Nanog and SSEA-1 in pre-iPSCs generated from MEFs$^{Nanog\text{-}GFP}$. (E^{I}) Expression of Wnt target genes analyzed by qPCR in pre-iPSCs$^{Nanog\text{-}GFP}$ grown in ESC medium, and ESC medium supplemented with Meki (PD0325901) ±Dkk1. (F^{I}) qPCR of pre-iPSCs $^{Nanog\text{-}GFP}$ and iPSCs $^{Nanog\text{-}GFP}$ to analyse the reactivation of stem cell specific genes. (G^{I}) Teratoma formed after injection of iPSCs $^{Nanog\text{-}GFP}$ were stained with H&E to identify tissues coming from different germ layers. (H^{I}) Immunofluorescence staining for Nestin (marker of ectoderm lineage), Smooth Muscle Actin (SMA, marker of mesoderm lineage) and FoxA2 (marker of endoderm lineage) using teratoma sections. (I^{I}) General scheme of iPSC generation protocol. Pre-iPSCs$^{Nanog\text{-}GFP}$(Nanog- and SSEA-1+) were infected with a lentiviral vector containing Nanog coding sequence. Drug selected clones were switched to ESC medium ±Dkk1 (50ng/mL). (J^{I}) iPSCs were analyzed for Nanog and Oct4 expression by immunofluorescence. (K^{I}) Percentage of fully reprogrammed Nanog-GFP+ iPSCs over total pre-iPS clones. (L^{I})

Pre-iPSCs $^{\beta\text{-cat fl/fl}}$characterization by immunofluorescence of SSEA-1, β-catenin and Nanog. (M^{l}) Western blot of total β-catenin using extracts of pre-iPSCs $^{\beta\text{-cat fl/fl}}$ ±tamoxifen. (N^{l}) Pre-iPSCs $^{\beta\text{-cat fl/fl}}$ treated with tamoxifen and grown in ESC medium plus Meki were stained for Nanog, Oct4, SSEA-1 and β-catenin. (O^{l}) Pre-iPSCs grown in ES medium without tamoxifen but in presence of Meki, converted into iPSCs, were characterized by immunofluorescence. Data are means ±SEM (n = 3). p >0.1, *, p <0.05, **, p <0.01, ***, p <0.0001. Scale bar, 25 μm (L, O, W, D^{l}, H^{l}, J^{l}, L^{l}, N^{l} and O^{l}). Scale bar, 100 μm (G^{l}). Scale bar, 200 μm (H, inset and B^{l}, inset). The immunofluorescence images in D^{l}, G^{l}, H^{l}, J^{l}, L^{l}, N^{l} and O^{l} were collected using a not confocal inverted microscope.

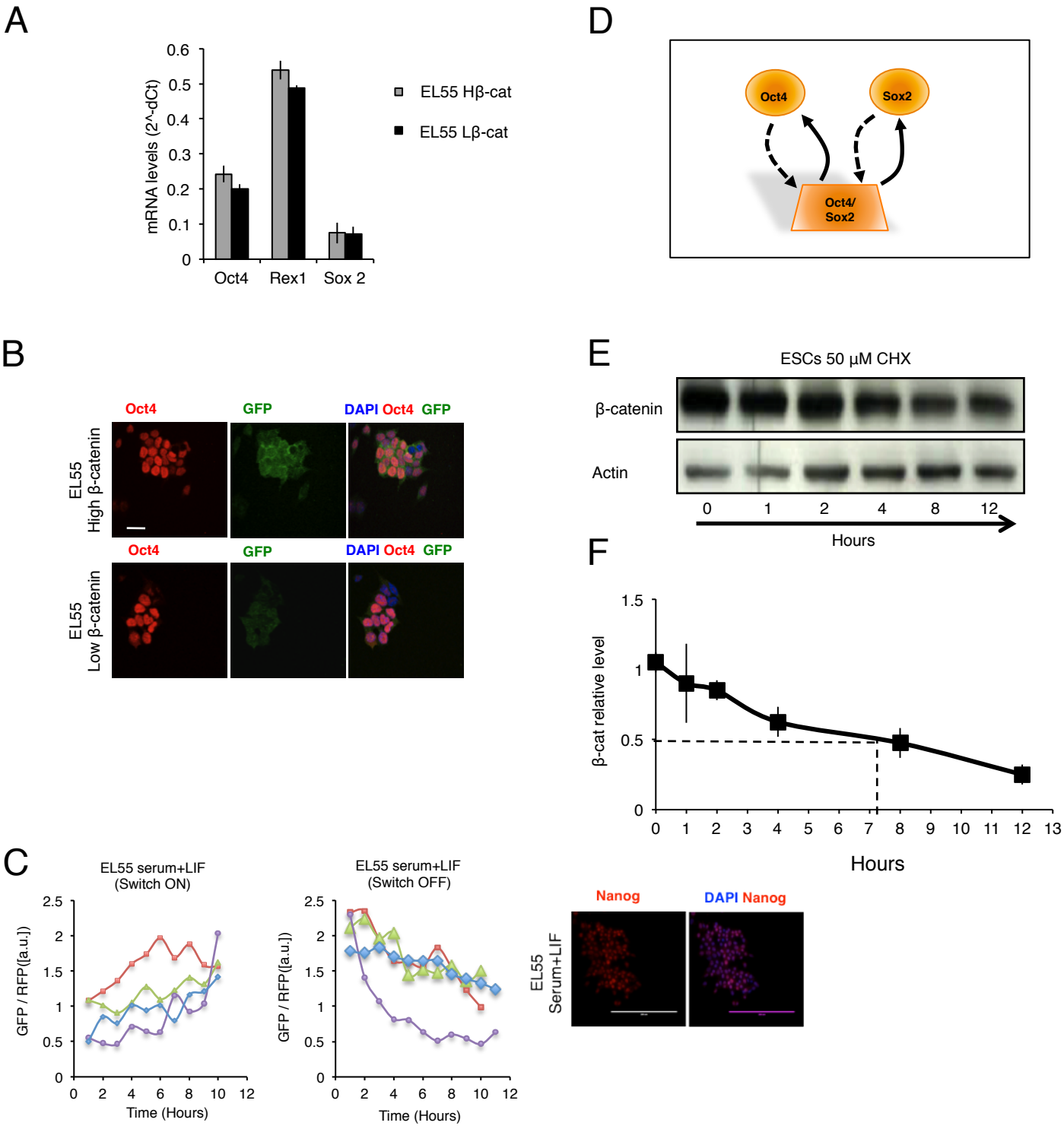

A
mRNA levels (2^-dCt)
0.6
0.5
0.4
0.3
0.2
0.1
0
Oct4
Rex1
Sox 2
EL55 Hβ-cat
EL55 Lβ-cat
D
Oct4
Sox2
Oct4/
Sox2
B
Oct4
GFP
DAPI Oct4 GFP
EL55
High β-catenin
EL55
Low β-catenin
E
ESCs 50 μM CHX
β-catenin
Actin
0
1
2
4
8
12
Hours
F
β-cat relative level
1.5
1
0.5
0
0 1 2 3 4 5 6 7 8 9 10 11 12 13
Hours
C
EL55 serum+LIF
(Switch ON)
EL55 serum+LIF
(Switch OFF)
GFP / RFP([a.u.])
2.5
2
1.5
1
0.5
0
0 2 4 6 8 10 12
Time (Hours)
Nanog
DAPI Nanog
EL55
Serum+LIF

Figure S3. Fluctuations of β-catenin and Nanog in mESCs cultured in serum+LIF medium, Related to Figure 3.

(A and B) qPCR of pluripotency genes and immunofluorescence of Oct4 and GFP using FACS-sorted L β-cat (GFP-) and H β-cat (GFP+) EL55 cells. (C) Quantification of the GFP signal normalized against the H2B-RFP signal in single cell time lapse imaging of EL55 cells cultured in serum+LIF medium. Switch on and off are shown. (C, right) Pluripotency of EL55 cells cultured in serum+LIF was not affected by laser exposure in cells analyzed at the end of time-lapse experiments by Nanog immunostaining. (D) Schematic representation of the Oct4/Sox2 heterodimer autoregulation. (E) ESCs were treated with cycloheximide (50 μM CHX) for 12 h, and the pelleted cells were analyzed by Western blotting. (F) Quantifican from Western blots. β-catenin protein levels were calculated by normalizing against actin. Dashed lines indicate β-catenin half-life. Data are means ±SEM (n = 3), p >0.1. Scale bar, 25 μm (B). Scale bar, 200 μm (C, right).

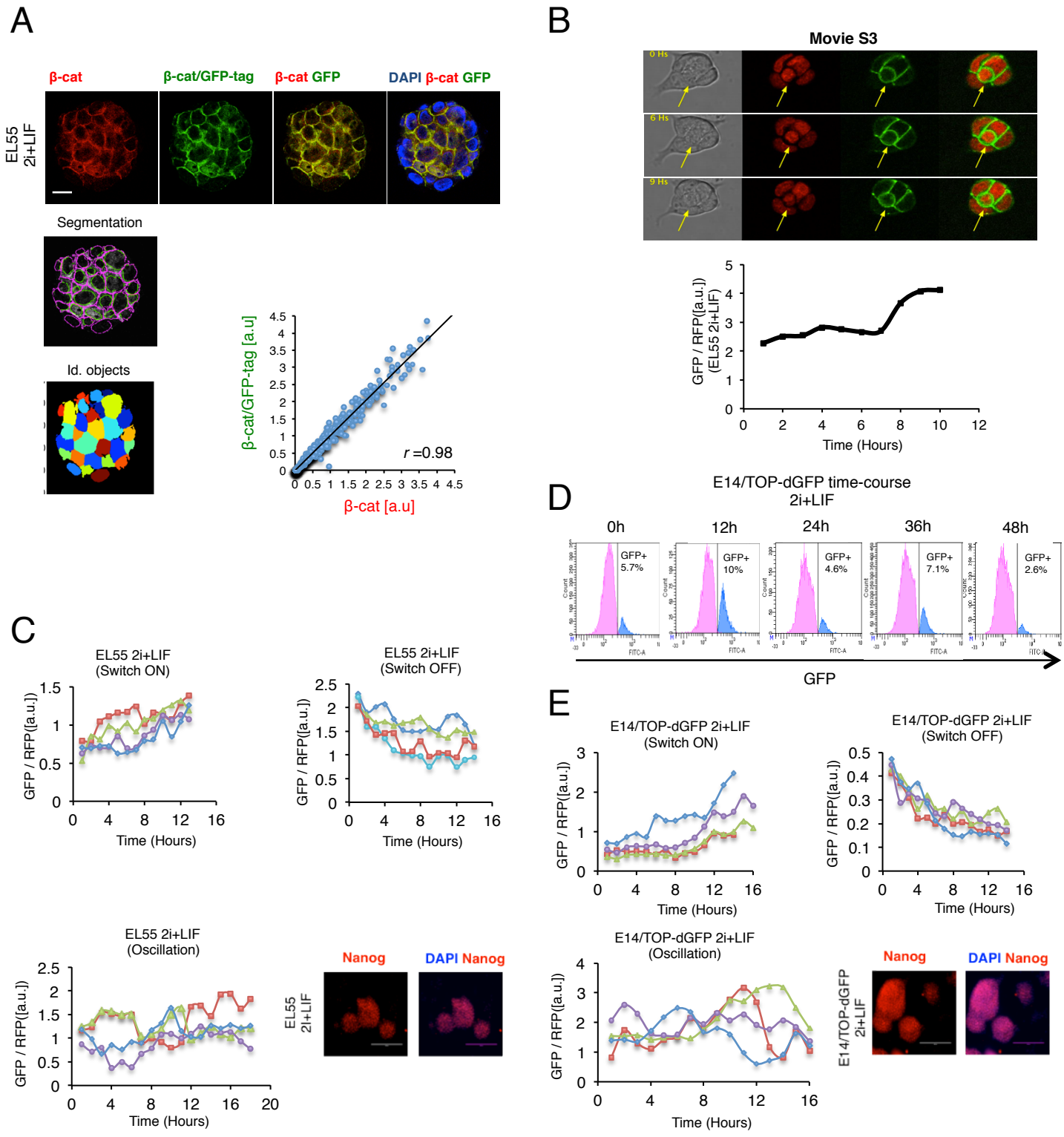

A
β-cat
β-cat/GFP-tag
β-cat GFP
DAPI β-cat GFP
EL55 2i+LIF
Segmentation
Id. objects
β-cat/GFP-tag [a.u]
β-cat [a.u]
r =0.98
B
Movie S3
0 Hs
6 Hs
9 Hs
GFP / RFP([a.u.]) (EL55 2i+LIF)
Time (Hours)
C
EL55 2i+LIF (Switch ON)
EL55 2i+LIF (Switch OFF)
EL55 2i+LIF (Oscillation)
GFP / RFP([a.u.])
Time (Hours)
Nanog
DAPI Nanog
EL55 2i+LIF
D
E14/TOP-dGFP time-course 2i+LIF
0h
12h
24h
36h
48h
GFP+ 5.7%
GFP+ 10%
GFP+ 4.6%
GFP+ 7.1%
GFP+ 2.6%
GFP
E
E14/TOP-dGFP 2i+LIF (Switch ON)
E14/TOP-dGFP 2i+LIF (Switch OFF)
E14/TOP-dGFP 2i+LIF (Oscillation)
GFP / RFP([a.u.])
Time (Hours)
Nanog
DAPI Nanog
E14/TOP-dGFP 2i+LIF

Figure S4. Fluctuations of β-catenin and Nanog in mESCs cultured in 2i+LIF, Related to Figure 4.

(A) Immunofluorescence of total β-catenin and GFP in EL55 cells cultured in 2i+LIF medium and correlation plot of β-catenin and GFP in EL55 cells (*r* is the Pearson correlation coefficient). Segmented images and identified objects are shown. (B) Snapshots of the movie S3 of EL55 cells cultured in 2i+LIF medium with relative quantification of the GFP signal normalized against the H2B-RFP signal. Yellow arrows indicate GFP switch on. (C) Quantification of the GFP signal normalized against the RFP in single cell time lapse imaging of EL55 cells cultured in 2i+LIF medium. Switch on, switch off and oscillations are shown. (C, right) Pluripotency of EL55 cells cultured in 2i+LIF was not affected by laser exposure in cells analyzed at the end of time-lapse experiments by Nanog immunostaining. (D) Representative FACS analysis of 48 hours time-course experiment of unsorted E14/TOP-dGFP grown in 2i+LIF. (E) Quantification of the GFP signal normalized against the H2B-RFP signal in single cell time lapse imaging of E14/TOP-dGFP cells cultured in 2i+LIF medium. Switch on, switch off and oscillations are shown. (E, right) Pluripotency of E14/TOP-dGFP cells cultured in 2i+LIF was not affected by laser exposure in cells analyzed at the end of time-lapse experiments by Nanog immunostaining. Data are means ±SEM (n = 3). Scale bar, 25 μm (A). Scale bar, 200 μm (C, inset and E, inset).

Supplemental Table 1. Parameters of the mathematical model; cell lines used in the present study; list of primers.

Supplemental Movies. β -catenin fluctuations in single cell live imaging, Related to Figures 3 and 4.

Movie S1. Time-lapse of the EL55 cells in serum+LIF medium. White arrow indicates GFP switch-off while the yellow arrow GFP indicates switch-on.

Movies S2 and S3. Time-lapses of the EL55 cells in 2i+LIF medium. White arrow indicates GFP switch-off while the yellow arrow indicates GFP switch-on.

Movie S4. Time-lapses of E14/TOP-dGFP cells in 2i+LIF medium. Yellow arrow that becomes white indicates an oscillation of the GFP signal while the yellow arrow from frame 4 onward indicates GFP switch-on.

EXTENDED EXPERIMENTAL PROCEDURES

Cell lines

ESCs were cultured on gelatin in knockout Dulbecco's modified Eagle's medium (DMEM) supplemented with 20% fetal bovine serum (Hyclone), 1 x nonessential amino acids, 1 x GlutaMax, 1 x 2-mercaptoethanol, and 1000 U/ml LIF ESGRO (Millipore). NPCs-Oct4-puro (kind gift of A. Smith) and TNGA ESCs (kind gift of I. Chambers) were generated and cultured as previously described (Chambers et al., 2007; Conti et al., 2005). NPCs-Oct4-puro cells were further modified by inserting the hygromycin-resistance gene under a constitutive promoter (pCAG). Cells were selected to create stable clones expressing the hygromycin-resistance gene. E14Tg2a and EF4 ESCs (kind gift of I. Chambers) were cultured as previously described (Chambers et al., 2003). The ESC mutants N1 and ΔN4 were derived from wild-type ESCs (β-catenin fl/fl) and β-catenin Δ/Δ cells, kind gift of C. Hartmann (Lyashenko et al., 2011). They were clonally isolated after nucleofection (Amaxa) of the pCAG-Nanog (kind gift of I. Chambers) and selected with puromycin. Wild-type RF8 ESCs, kind gift of R. Farese, were described in (Meiner et al., 1996). Nanog βgeo/+ cells and Nanog βgeo/Hygro (kind gift of S. Yamanaka) were genetically derived as previously described (Mitsui et al., 2003).

EL55 ESCs (Sv/129 background) were obtained by inserting a GFP-tag in the endogenous β-catenin locus gene using Zinc Finger technology (Isalan et al., 2001). The EL55 clone was selected for GFP integration via single cell sorting by FACS. Sorted GFP-positive cells were then expanded and genomic DNA was used to identify the clones in which GFP had recombined with the endogenous β-catenin gene. E14-TOP-dGFP cells were clonally isolated from wild-type E14Tg2a cells nucleofected with a TOP-dGFP plasmid (destabilized GFP was inserted in the 7TGP plasmid (Addgene) to replace the original enhanced GFP), and drug selected.

Cells used in time-lapse experiments (EL55 and E14-TOP7x-dGFP) were stably nucleofected with pHIV-H2BmRFPplasmid purchased from Addgene (Plasmid 18982) (Welm et al., 2008) carrying a H2BmRFP sequence.

Dkk1 was silenced by infecting cells with viral ShRNA against Dkk1 (Sigma, MISSION shRNA, TCR number TRCN0000055155, clone ID NM_010051.2-228s1c1) and with ShControl (pLKO.1 puro, Sigma). Infected cells were drug selected for the integration of the virus before fusion experiment.

Drug treatments

EF4 cells (1.0 x10^6) were plated on gelatin and treated for 24 h with 50 ng/mL Dkk1 recombinant protein (R&D Systems). IWP2 (Stemgent) was used at 2 μM, during 24 hour treatment. RF8 cells (1.0 x10^6) and Nanog βgeo/+ cells (1.0 x10^6) were plated on gelatin and treated for 24 h with CHIR99021(3 μM) (Selleck Chemicals) (Bain et al., 2007). Similarly, recombinant Wnt3a protein (R&D) was used at 200 ng/ml (48 hours treatment). Twenty-four hours later, cells were trypsinized, counted and plated on NPCs for fusion, or harvested for RNA and protein analyses. Fusions and drug selection were performed as described in the Cell hybrids protocol. For the fusion of RF8 and Nanog βgeo/+ cells, the hybrids were treated additionally for 72 h with CHIR99021 before starting drug selection.

EL55 and ESC-TNGA cells were treated with 3 μM CHIR99021 and 3 μM Mek inhibitor (PD184352, Sigma) (Davies et al., 2000) for 1 day and 7 days, respectively. After each treatment cells were collected and analyzed by flow cytometry. PD184352 was refreshed every 48 hours.

Western blotting

Western blotting was performed as previously described (Zito et al., 2007). The primary antibodies used were: anti-β-catenin, clone 14 (BD Biosciences), working concentration 1:1000; anti-Nanog (CALBIOCHEM), working concentration 1:1000; anti-β-actin (Abcam), working concentration 1:2000; anti-GFP (Santa Cruz Biotechnology), working concentration 1:500; anti-Dkk1 (Santa Cruz Biotechnology), working concentration 1:100; anti-Plakoglobin (BD Biosciences), working concentration 1:1000; anti E-Cadherin (BD Biosciences), working concentration 1:1000; anti-Oct3/4 (Santa Cruz Biotechnology), working concentration 1:1000. The secondary antibodies were diluted 1:3000.

Immunostaining

Cells were washed twice with phosphate-buffered saline (PBS), fixed with 4% paraformaldehyde for 15 min at RT, and blocked in PBS with 0.3% Triton X-100 and 10% goat serum, for 60 min. The cells were incubated with the specific primary antibodies for 4 h, and 1 h with the secondary antibody conjugated with fluorescein. The cells were then washed and mounted on slides with a few drops of Vectashield, with DAPI (Vector Laboratories).

The primary antibodies used for immunostaining were: anti-β-catenin, clone 14 (BD Biosciences), working concentration 1:1000; anti-active-β-catenin (ABC), working concentration 1:400, clone 8E7 (Millipore); anti-GFP (Santa Cruz Biotechnology), working concentration 1:1000; anti-SSEA-1, clone 480 (Santa Cruz Biotechnology), working concentration 1:500; anti-Nanog (CALBIOCHEM), working concentration 1:500; anti-Oct3/4, clone C10 (Santa Cruz Biotechnology), working concentration 1:1000; anti-Nestin (Abcam), working concentration 1:200; anti-FoxA2 (ab40874 Abcam), working concentration 1:400; anti-Smooth-Muscle-Actin (SMA, Sigma), working concentration 1:400; anti-Plakoglobin (BD Biosciences), working concentration 1:400; anti E-Cadherin (BD Biosciences), working concentration 1:400; anti-EEA1 (BD Biosciences), working concentration 1:50. The fluorescent conjugated secondary antibodies were diluted 1:1000.

Immunostaining quantification and correlation analysis

To indentify single-cell (segmentation) in immunostainings, we implemented an automated methodology using CellProfiler (Carpenter et al., 2006). The designed pipeline detects nuclei from DAPI, propagates nuclei to indentify cytoplasm, quantify fluorescence on the indentified objects (pipeline available upon request). Over-segmented or under-segmented objects were removed manually where needed. Line plot distribution, scatterplots and Pearson correlation coefficient were generated using Excel.

qPCR

For quantitative PCR, the total RNA was extracted from mouse ESCs, MEFs, Pre-iPSCs and iPSCs using the RNeasy kit (Qiagen), and the cDNA was generated from 1 µg of RNA using Superscript III (Invitrogen). For cDNA 25 ng was used as template for each reaction, in a10 µl reaction volume. LightCycler 480 SYBR Green I Master (Roche) was used with LightCycler®480 System (Roche).

Chromatin immunoprecipitation assay

Chromatin immunoprecipitation (ChIP) was carried out using the protocol described in (Morey et al., 2012). ESCs were trypsinised and crosslinked in 1% formaldehyde for 10 min at room temperature. The crosslinking was quenched with 0.125 M glycine for 5 min. The pelleted cells were lysed in 1 ml ChIP buffer and sonicated for 10 min in a Bioruptor sonicator (Diagenode). The soluble material was quantified using Bradford assays. To immunoprecipitate the transcription factors, 1mg protein was used, and 5 µg anti-Nanog (BETHYL laboratories) and 5 µg IgG were incubated overnight with the chromatin. The immunocomplexes were recovered with 30 µl protein A or G agarose bead slurries. The immunoprecipitated material was washed three times with a low-salt buffer, and one time with a high-salt buffer. DNA complexes were decrosslinked at 65 °C for 3 h, and the DNA was then eluted in 200 µl water using the PCR purification kit (QIAGEN). Two microliters DNA was used for each qPCR reaction.

FACS analysis and cell sorting

After CHIR99021 and Mek inhibitor treatment, the untreated and treated ESCs were trypsinized and the pelleted cells were resuspended in PBS with 2% FBS with DAPI. The endogenous GFP of the EL55 and TNGA cells was analysed using a BD LSR Fortessa. For FACS sorting, cells were prepared in the same way and sorted on a BD FACS aria II. To check cell fusion efficiency, NPCs and ESCs were stained with Mito Tracker, from Invitrogen, green (300 nM) and orange (150 nM) respectively, and incubated at 37°C for 30 min. The day after, green NPCs and orange ESCs were co-cultured as described in the cell hybrids section. Mito Tracker signal was analyzed using a BD LSR Fortessa 4 hours after fusion.

EL55 cell generation with zinc finger technology

A genomic target region was chosen to provide a G-rich, stop-codon free, in-frame sequence, close to the N-terminus of β-catenin. Zinc fingers were designed rationally with the help of ZiFit (Sander et al., 2012). DNA recognition helix design was guided by (Isalan et al., 2001). To form functional obligate heterodimer zinc finger nucleases (ZFNs), DNA for zinc finger proteins (ZFPs) was synthesised and cloned via XbaI/BamHI into pMLM290/pMLM292 expression plasmids (Miller et al., 2007), (http://www.addgene.org/21873/ and http://www.addgene.org/21872/).

ZFP-FokI DNA coding sequences (Zinc finger a-helices underlined):

>bCat_1LEFT_3F_pMLM290

ATGGGACCTAAGAAAAAGAGGAAGGTGGCGGCCGCTGACTACAAGGATG
ACGACGATAAATCTAGACCCGGGGAGCGCCCCTTCCAGTGTCGCATTTGC
ATGCGGAACTTTTCGACCACCGGCGCCCTGACCGAACATACCCGTACTCA
TACCGGTGAAAAACCGTTTCAGTGTCGGATCTGTATGCGAAATTTCTCCCG
CAGCTCCAACCTGACCAGGCATCTACGTACGCACACCGGCGAGAAGCCAT
TCCAATGCCGAATATGCATGCGCAACTTCAGTCAGAGCTCCGACCTGACC
CGCCACCTAAAAACCCACCTGAGGGGATCCCTAGTCAAAAGTGAACTGGA
GGAGAAGAAATCTGAACTTCGTCATAAATTGAAATATGTGCCTCATGAAT
ATATTGAATTAATTGAAATTGCCAGAAATTCCACTCAGGATAGAATTCTTG
AAATGAAGGTAATGGAATTTTTTATGAAAGTTTATGGATATAGAGGTAAA
CATTTGGGTGGATCAAGGAAACCGGACGGAGCAATTTATACTGTCGGATC
TCCTATTGATTACGGTGTGATCGTGGATACTAAAGCTTATAGCGGAGGTTA
TAATCTGCCAATTGGCCAAGCAGATGAAATGCAACGATATGTCAAAGAAA
ATCAAACACGAAACAAACATATCAACCCTAATGAATGGTGGAAAGTCTAT
CCATCTTCTGTAACGGAATTTAAGTTTTTATTTGTGAGTGGTCACTTTAAA
GGAAACTACAAAGCTCAGCTTACACGATTAAATCATAAGACTAATTGTAA
TGGAGCTGTTCTTAGTGTAGAAGAGCTTTTAATTGGTGGAGAAATGATTA
AAGCCGGCACATTAACCTTAGAGGAAGTGAGACGGAAATTTAATAACGGC
GAGATAAACTTTTAA

>bCat_1RIGHT_pMLM292

ATGGGACCTAAGAAAAAGAGGAAGGTGGCGGCCGCTGACTACAAGGATG
ACGACGATAAATCTAGACCCGGGGAGCGCCCCTTCCAGTGTCGCATTTGC
ATGCGGAACTTTTCGCGCAGCGACGCCCTGACCAGGCATACCCGTACTCA
TACCGGTGAAAAACCGTTTCAGTGTCGGATCTGTATGCGAAATTTCTCCCA
GAGCTCCGACCTGAGCCGCCATCTACGTACGCACACCGGCGAGAAGCCAT
TCCAATGCCGAATATGCATGCGCAACTTCAGTCAGAGCTCCGACCTGACC
CGCCACCTAAAAACCCACCTGAGGGGATCCCAACTAGTCAAAAGTGAACT
GGAGGAGAAGAAATCTGAACTTCGTCATAAATTGAAATATGTGCCTCATG
AATATATTGAATTAATTGAAATTGCCAGAAATTCCACTCAGGATAGAATT
CTTGAAATGAAGGTAATGGAATTTTTTATGAAAGTTTATGGATATAGAGG
TAAACATTTGGGTGGATCAAGGAAACCGGACGGAGCAATTTATACTGTCG
GATCTCCTATTGATTACGGTGTGATCGTGGATACTAAAGCTTATAGCGGAG
GTTATAATCTGCCAATTGGCCAAGCAGATGAAATGGAGCGATATGTCGAA
GAAAATCAAACACGAAACAAACATCTCAACCCTAATGAATGGTGGAAAG
TCTATCCATCTTCTGTAACGGAATTTAAGTTTTTATTTGTGAGTGGTCACTT
TAAAGGAAACTACAAAGCTCAGCTTACACGATTAAATCATATCACTAATT
GTAATGGAGCTGTTCTTAGTGTAGAAGAGCTTTTAATTGGTGGAGAAATG
ATTAAAGCCGGCACATTAACCTTAGAGGAAGTGAGACGGAAATTTAATAA
CGGCGAGATAAACTTTTAA

ZFN Protein Sequences

Zinc finger a-helices are underlined. Sequences include FokI (positively or negatively charged) from pMLM290/pMLM292, N-terminal Nuclear Localisation Signals (NLS) and FLAG-tag:

>bCat_1LEFT_3F_pMLM290-FokI+

MGPKKKRKVAAADYKDDDDKSRPGERP
FQCRICMRNFSTTGALTEHTRTHTGEKP
FQCRICMRNFSRSSNLTRHLRTHTGEKP
FQCRICMRNFSQSSDLTRHLKTHLRGS

LVKSELEEKKSELRHKLKYVPHEYIELIEIARNSTQDRILEMKVMEFFMKVYG
YRGKHLGGSRKPDGAIYTVGSPIDYGVIVDTKAYSGGYNLPIGQADEMQRYV
KENQTRNKHINPNEWWKVYPSSVTEFKFLFVSGHFKGNYKAQLTRLNHKTN
CNGAVLSVEELLIGGEMIKAGTLTLEEVRRKFNNGEINF*

>bCat_1RIGHT_pMLM292-FokI-

MGPKKKRKVAAADYKDDDDKSRPGERP

FQCRICMRNFSRSDALTRHTRTHTGEKP

FQCRICMRNFSQSSDLSRHLRTHTGEKP

FQCRICMRNFSQSSDLTRHLKTHLRGS

QLVKSELEEKKSELRHKLKYVPHEYIELIEIARNSTQDRILEMKVMEFFMKVY
GYRGKHLGGSRKPDGAIYTVGSPIDYGVIVDTKAYSGGYNLPIGQADEMERY
VEENQTRNKHLNPNEWWKVYPSSVTEFKFLFVSGHFKGNYKAQLTRLNHIT
NCNGAVLSVEELLIGGEMIKAGTLTLEEVRRKFNNGEINF*

iPSC generation

Pre-iPSCs were generated by retroviral infection of MEFs with pMXs-based containing the four factors: Oct4, Sox2, c-Myc and Klf4 obtained from Addgene, Inc. The plasmids containing the four factors were transfected into the Platinum-E Retroviral Packaging cell line, Ecotropic from Cell Biolabs Inc packaging cell line (ref.RV-101) using the CalPhos™ Mammalian Transfection kit from Clontech Laboratories, Inc. (ref.631312). Then 48 hours before transfection, 5 x10^4 murine embryonic fibroblasts (MEFs) were seeded in each well of a 6-well plate. The virus-containing supernatants were supplemented with 4 mg/ml of polybrene. Equal amounts of viral supernatants containing each of the 4 retroviral vectors were mixed, added to the MEFs and incubated overnight. The cells were treated with the viral supernatants two more times. At 48 h after the last infection, the cells were switched to ESC medium supplemented with 1,000 U/ml of leukemia inhibitory factor (LIF). Two days after switching the medium, the infected fibroblasts were harvested by trypsinization and each well was replated into a 100-mm dish on MEF feeder layers. The medium was replaced every day.

Pre-iPSCs from MEFs purified from a Nanog-GFP mouse strain (Tg(Nanog-GFP,Puro)1Yam, Riken), were switched into ESC medium plus MEK Inhibitor (PD0325901, Selleck Chemicals, 1 μM) containing or not Dkk1 recombinant protein. Seven days after switching medium, iPSCs (Nanog-GFP positive) were counted.

Pre-iPSCs from MEFs purified from a Nanog-GFP mouse strain (Tg(Nanog-GFP,Puro)1Yam, Riken) were infected with pBABE-Nanog-Hygro virus (Nanog coding sequence was cloned into pBABE-Hygro plasmid, purchased by Addgene) or with PBabe-Hygro virus as control. Infected cells were selected for the virus integration for three days. After three additional days, Dkk1 was added or not to ESC medium, and five days later iPSCs (Nanog-GFP positive) were counted.

Pre-iPSCs from MEFs purified from the B6.129-Ctnnb1tm2Kem/KnwJ/β-Actin-CRE mouse strain (β-catenin conditional KO, inducible with tamoxifen from Jackson Laboratories) were treated with 1 μM tamoxifen (Sigma) for 48 h, to excide the β-catenin gene and then switched to ESC medium containing MEK inhibitor (PD0325901, Selleck Chemicals, 1 μM) to promote iPSCs formation by Nanog overexpression. Control plates were incubated for 48 h with ethanol (vehicle for tamoxifen). Eight days after switching the medium, iPSCs Nanog+ were counted.

ELISA assay

Dkk1 dosage was carried out using the Quantikine mouse Dkk-1 Immunoassay from R&D (MKK100). Cell culture supernatant collected from wild-type ESCs and mutant ESCs was incubated with the appropriate antibodies according to the manufacturer. A standard curve was generated plotting on the y-axis the optical density of each standard and on the x-axis the relative concentration. Dkk1 concentration in pg/mL was calculated fitting the calibration curve.

Teratoma production

Cells were trypsinized into single-cell suspensions and resuspended in phosphate-buffered saline to a concentration of 1.5 $x10^7$ cells/mL. These cells were injected subcutaneously into Fox Chase SCID mice using a 25 gauge needle (200 ml).

Teratomas were collected after 4 weeks and were fixed, embedded, sectioned, and stained for Nestin (1:200), FoxA2 (1:400) and SMA (1:400).

Mathematical model derivation

The mathematical model is composed of four differential equations for the Oct4/Sox2, Nanog, Dkk1 and β-catenin concentrations. They are derived from stoichiometric equations for transcription factors binding to the genes. The main assumptions of the model are: (a) the concentration of the Oct4 and Sox2 heterodimer is in dynamic equilibrium with the ones of Oct4 and Sox2, thus the concentrations of the single proteins can be neglected; (b) post-transcriptional interactions can be ignored, considering just the transcriptional ones; (c) Nanog is mainly regulated by the Oct4-Sox2 heterodimer, and by itself; (d) Dkk1 is inhibited by Nanog; (e) β-catenin is directly inhibited by Dkk1; (f) activation and repression are Hill-like functions; (g) the decays rates are first order. Bistability is given by the presence of Nanog auto-positive feedback loop (Siciliano et al., 2013; Siciliano et al., 2011).

Time-lapse imaging confocal specifications

Time-lapse images were acquired on a Leica SP8 AOBS confocal laser scanning microscope attached to a Leica DM I6000 inverted epifluorescence microscope using Adaptive Focus Control to correct focus drift during time-courses and hybrid (GaAsP) detectors to increase sensitivity.

Statistical Analysis

Differences between groups were analyzed by Student *t* test. A *p*-value lower than 0.05 was considered statistically significant.

SUPPLEMENTAL REFERENCES

Bain, J., Plater, L., Elliott, M., Shpiro, N., Hastie, C.J., McLauchlan, H., Klevernic, I., Arthur, J.S., Alessi, D.R., and Cohen, P. (2007). The selectivity of protein kinase inhibitors: a further update. Biochem J *408*, 297-315.

Carpenter, A.E., Jones, T.R., Lamprecht, M.R., Clarke, C., Kang, I.H., Friman, O., Guertin, D.A., Chang, J.H., Lindquist, R.A., Moffat, J.*, et al.* (2006). CellProfiler: image analysis software for identifying and quantifying cell phenotypes. Genome Biol *7*, R100.

Chambers, I., Colby, D., Robertson, M., Nichols, J., Lee, S., Tweedie, S., and Smith, A. (2003). Functional expression cloning of Nanog, a pluripotency sustaining factor in embryonic stem cells. Cell *113*, 643-655.

Chambers, I., Silva, J., Colby, D., Nichols, J., Nijmeijer, B., Robertson, M., Vrana, J., Jones, K., Grotewold, L., and Smith, A. (2007). Nanog safeguards pluripotency and mediates germline development. Nature *450*, 1230-1234.

Conti, L., Pollard, S.M., Gorba, T., Reitano, E., Toselli, M., Biella, G., Sun, Y., Sanzone, S., Ying, Q.L., Cattaneo, E.*, et al.* (2005). Niche-independent symmetrical self-renewal of a mammalian tissue stem cell. PLoS Biol *3*, e283.

Davies, S.P., Reddy, H., Caivano, M., and Cohen, P. (2000). Specificity and mechanism of action of some commonly used protein kinase inhibitors. Biochem J *351*, 95-105.

Isalan, M., Klug, A., and Choo, Y. (2001). A rapid, generally applicable method to engineer zinc fingers illustrated by targeting the HIV-1 promoter. Nat Biotechnol *19*, 656-660.

Lyashenko, N., Winter, M., Migliorini, D., Biechele, T., Moon, R.T., and Hartmann, C. (2011). Differential requirement for the dual functions of beta-catenin in embryonic stem cell self-renewal and germ layer formation. Nat Cell Biol *13*, 753-761.

Miller, J.C., Holmes, M.C., Wang, J., Guschin, D.Y., Lee, Y.L., Rupniewski, I., Beausejour, C.M., Waite, A.J., Wang, N.S., Kim, K.A.*, et al.* (2007). An improved zinc-finger nuclease architecture for highly specific genome editing. Nat Biotechnol *25*, 778-785.

Morey, L., Pascual, G., Cozzuto, L., Roma, G., Wutz, A., Benitah, S.A., and Di Croce, L. (2012). Nonoverlapping functions of the Polycomb group Cbx family of proteins in embryonic stem cells. Cell Stem Cell *10*, 47-62.

Sander, J.D., Maeder, M.L., Reyon, D., Voytas, D.F., Joung, J.K., and Dobbs, D. (2012). ZiFiT (Zinc Finger Targeter): an updated zinc finger engineering tool. Nucleic Acids Res *38*, W462-468.

Siciliano, V., Garzilli, I., Fracassi, C., Criscuolo, S., Ventre, S., and di Bernardo, D. (2013). MiRNAs confer phenotypic robustness to gene networks by suppressing biological noise. Nature communications *4*, 2364.

Siciliano, V., Menolascina, F., Marucci, L., Fracassi, C., Garzilli, I., Moretti, M.N., and di Bernardo, D. (2011). Construction and modelling of an inducible positive feedback loop stably integrated in a mammalian cell-line. PLoS Comput Biol *7*, e1002074.

Welm, B.E., Dijkgraaf, G.J., Bledau, A.S., Welm, A.L., and Werb, Z. (2008). Lentiviral transduction of mammary stem cells for analysis of gene function during development and cancer. Cell Stem Cell *2*, 90-102.

Wray, J., Kalkan, T., Gomez-Lopez, S., Eckardt, D., Cook, A., Kemler, R., and Smith, A. (2011). Inhibition of glycogen synthase kinase-3 alleviates Tcf3 repression of the pluripotency network and increases embryonic stem cell resistance to differentiation. Nat Cell Biol *13*, 838-845.

Zito, E., Buono, M., Pepe, S., Settembre, C., Annunziata, I., Surace, E.M., Dierks, T., Monti, M., Cozzolino, M., Pucci, P.*, et al.* (2007). Sulfatase modifying factor 1 trafficking through the cells: from endoplasmic reticulum to the endoplasmic reticulum. Embo J *26*, 2443-2453.